ACCESS
Arctic Climate Change
Economy and Society

Project no. 265863

ACCESS

Arctic Climate Change, Economy and Society

Instrument: Collaborative Project

Thematic Priority: Ocean.2010-1 "Quantification of climate change impacts on economic sectors in the Arctic"

D2.51 – Design and fabrication of lateral stress sensor and measuring lateral stresses in Arctic sea ice

Due date of deliverable: **31/08/2014**

Actual submission date: **13/03/2015**

Start date of project: **March 1st, 2011** Duration: **48 months**Organisation name of lead contractor for this deliverable: **HSVA**

Project co-funded by the European Commission within the Seventh Framework Programme (2007-2013)		
Dissemination Level		
PU	Public	X
PP	Restricted to other programme participants (including the Commission Services)	
RE	Restricted to a group specified by the consortium (including the Commission Services)	
CO	Confidential, only for members of the consortium (including the Commission Services)	

D2.51 – Design and fabrication of lateral stress sensor and measuring lateral stresses in Arctic sea ice

By

Karl Ulrich-Evers & Peter Jochmann

Hamburgische Schiffbau-Versuchsanstalt (HSVA)

Jeremy Wilkinson

British Antarctic Survey (NERC-BAS)

Formally at Scottish Association for Marine Science (SAMS)

Philipp Hinse

Technical University Hamburg-Harburg (TUHH)

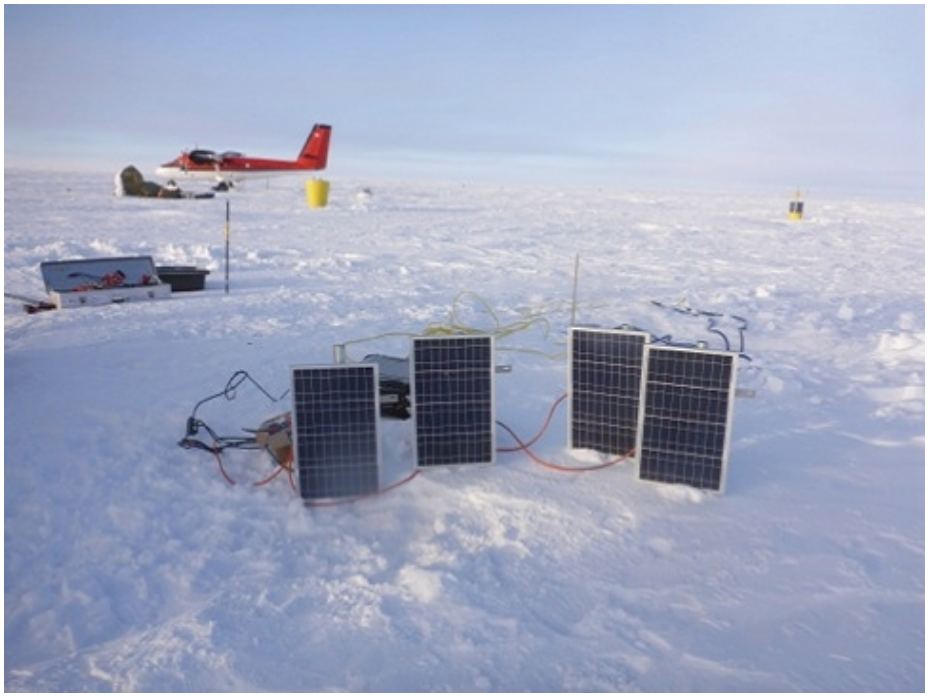

ACCESS is a 4 year European program (2011-2015) supported within the Oceans of Tomorrow call of the European Commission Seventh Framework Programme.
For further information about ACCESS please visit our website at www.access-eu-org

Document Control Sheet

Customer	:	**European Commission within the Seventh Framework Programme**
Project	:	**ACCESS - Arctic Climate Change, Economy and Society**
Project No.	:	**EU Project no. 265863**
Deliverable.	:	**D 2.51**
Report Title	:	**D 2.51 – Design and fabrication of lateral stress sensor and measuring lateral stresses in Arctic sea ice**
HSVA Order No.	:	**62.7061/524**
File	:	**EU-ACCESS_Final_D2.51_HSVA_v1.2**

Rev. No.	Date	Reason for Issue	Prepared by	Checked by	Approved by
1.2	Jan. 2015	Minor editorial changes executed	K.-U. Evers (HSVA)		
1.1	Jan. 2015	Status: Final version Delivery to ACCESS co-ordinator and WP 4 leaders for review - comments from reviewers are incorporated editorial improvements executed	K.-U.Evers (HSVA)		
1.0	Dec. 2014	Status: Draft D 2.51 – Design and fabrication of lateral stress sensor and measuring lateral stresses in Arctic sea ice Delivery to ACCESS co-ordinator and WP 2 leader for review	K.-U.Evers (HSVA) P. Jochmann (HSVA) J. Wilkinson (BAS) P. Hinse (TUHH)		

Keywords: **Arctic sea ice, Arctic shipping, lateral ice pressure, ice stress measurements,**

Contents

List of Figures

Executive Summary

The Hamburg Ship Model Basin (HSVA) together with the Scottish Association of Marine Science (SAMS) has developed in cooperation with Terrascience Systems Ltd., Canada an ice stress sensor system to be frozen in level or pack ice in the Arctic during the ACCESS WP 1 expedition organised by SAMS.

The objectives were to get lateral ice pressure data together with environmental information, temperature, wind speed and direction, current etc. and position of the ice stress sensors that should be transmitted via satellite onshore. Available meteorological and oceanographic data and satellite pictures should be used to gather information on the dependence of the ice pressure on environmental parameters. The goal was to use the collected data for improvement of the ICEROUTE- transit model. In WP1 the data should be used to benchmark the ice prediction models with respect to ice pressure.

During the design phase of the Lateral Stress Buoy (LSB), it became evident that the production of the measurement system is too expensive. Due to the high weight of the LSB, problems regarding transportation, handling and insertion into the ice, high costs were expected. It was also recognized that timely completion could not be guaranteed. For these reasons, it was decided in consultation with the leader of WP 2, not to pursue the development of this measurement system and to search for an alternative.

As an alternative ice force panels (IFP) from the company Terrasciences Ltd. in Canada were selected. About this idea the European Commission, Directorate-General for Research and Innovation was informed and a reallocation of funds for production of equipment in Task 2.51 has been requested. This application was approved by the EU scientific officer, who is responsible for the collaborative ACCESS Project no. 265863 – Arctic Climate Change, Economy and Society.

The IDEAL ice force panels (IFP) are custom-made manufactured according to the specifications given by HSVA and should be used during the Arctic Expedition Winter 2013/14 in Fram Strait with research vessel RV Lance.

The plan was to use the ice force panels during the expedition towards northeast Spitsbergen where RV Lance will freeze in level or pack ice and move with the transpolar drift towards the Fram Strait.

Based on a decision of the Norwegian Research Council, the expedition could not be performed. This message was achieved during the ACCESS General Assembly meeting in Villanova in March 2013 and it was decided to use the IDEAL IFP during the Ice Camp field campaign in the Beaufort Sea in March 2014 organized by SAMS. The equipment was shipped to Sachs Harbour, Canada and deployed in sea ice by SAMS.

A fault in the internal SD card-holder of IFP data acquisition unit meant that no data was recorded during the Ice Camp field campaign. This is particularly disappointing because on the one hand it was possible to design and produce the ice stress measurement system and on the other hand, all constructive, technical, and logistical preparations were carried out for this Ice Camp campaign with huge effort to investigate the lateral pressure in Arctic sea ice.

In addition, a literature review regarding lateral ice pressure, which was not originally part of the ACCESS WP 2 Task 2.51 was performed.

The results of the literature study can be summarized briefly: In various field measurements campaigns carried out in Arctic sea ice (e.g. Beaufort Sea, Lancaster Sound and Spitsbergen) lateral ice pressure in the range of p = 150 kPa to 300 kPa was determined.

Because there is still too little information about temporal and spatial evolution of the ice pressure field, it is highly recommended to perform interdisciplinary field campaigns with geophysicists, meteorologists, oceanographers and ice engineers in the Arctic in the future.

In such a campaign a better understanding of the lateral pressure of the ice can be obtained by use of complementary data sets.

New insights can be gained to what extent the climatic development in the Arctic in recent years has affected the internal pressure of the ice these days.

1 Introduction

Ice-going ships and offshore structures may need to operate in a wide range of various ice conditions, ranging from continuous level ice to, multi-year ice floes pack ice fields and pressure ridges. Compressive pack ice condition is a severe obstacle to safe and effective navigation in ice covered waters. On the one hand pack ice can hinder the ship transit and the maneuverability of a vessel and on the other hand considerable damage to the ship or the loss can be caused by pack ice forces due to polar pack ice movement.

The knowledge of magnitude of internal stress in an ice sheet is important because it is considered as a basic requirement for the development of methods and indexes for forecasting pressured ice applied on vessels and offshore structures (Abdelnour, 1997).

A number of field measurements In the Beaufort Sea and along the Labrador coast were carried out in the period 1989-1993 in order to determine the stress in multi-year ice floes, in land-fast ice and pack ice.

The results from these field campaigns are valuable for developing a general understanding of pack ice pressures as they contain information about ice forces and ice pressures generated associated with ice and environmental conditions.

Furthermore the analyzed results show that stress measurements are related to the regional deformation behavior of the ice cover and confirm that regional-scale ice dynamics is primarily a function of coastal geometry and sustained, large-scale wind direction and magnitude (*Richter-Menge et al., 2002*).

Direct measurements of ice stress in field campaigns provide a valuable contribution for the development of design rules for ice-going vessels and for a probabilistic load calculation procedure for structure design. In addition, ice stress parameters provide valuable information for the numerical simulation of climate models.

We have recently witnessed significant changes in all aspects of the Arctic marine environment, especially the sea ice. These changes in the sea ice cover have occurred over a handful of years, and our current knowledge of ice mechanics and

dynamics stems largely from observations in a multi-year ice setting, rather than the first-year ice dominated Arctic we find today. The extraordinary reduction in sea-ice extent and thickness influences fundamental sea ice properties, including dynamics, mechanics and thermodynamics. It therefore calls into question our current state of knowledge of these processes, and the validity of many of the parameterisations presently embedded in coupled sea ice models. Previous data has shown that first-year ice loads are on the order of 100 MN, but more high quality data is needed to improve our understanding of ice forces (*Dempsey, 2000*).

Detailed ice mechanics and dynamics research has been performed in the Arctic since oil exploration began in the 1970s. Both industry and government continued to invest in ice mechanics research during the 1980s and 1990s, but since this time research in this field has tailored off. In the early to mid-1990s ONR, through the Sea Ice Mechanics Initiative (SIMI), funded a 5-year program whose goal was to understand sea ice constitutive laws and fracture mechanics over the full range of geophysical scales (centimetres to kilometres). Whilst significant gains have been made over the years our knowledge is incomplete. This has mainly been due to complex and changing nature of properties associated with sea ice, along with a lack of continuous, high resolution, data on the key parameters.

2 Objectives

The Hamburg Ship Model Basin (HSVA) together with the Scottish Association of Marine Science (SAMS) has developed an ice stress sensor system to be frozen in level or pack ice in the Arctic during the ACCESS WP 1 expedition organised by SAMS.

The measured lateral ice pressure data together with environmental information, temperature, wind speed and direction, current etc. and position of the ice stress sensors should be transmitted via satellite onshore. Available meteorological and oceanographic data and satellite pictures should be used to gather information on

the dependence of the lateral ice pressure on environmental parameters. The collected data should be used to improve the ICEROUTE- transit model. In WP1 the data should be used to benchmark the ice prediction models with respect to ice pressure.

3 Design of a Lateral Stress Buoy (LSB)

In developing the "lateral stress buoy" (LSB) it was investigated to what extent the possibility exists to employ a cylinder, which was used as an offshore model in the ice tank at HSVA. To determine this, a FEM model was created and two different load cases simulated. The calculations were performed using the software MSC Marc-Mentat 2010. To continue using the cylinder as a LSB only elastic deformations are allowed. For this reason, only linear elastic FEM calculations were performed.

3.1 Description of the cylinder

The existing S235JR steel cylinder has a height of H = 3000 mm and a diameter of D = 1150 mm (Figure 1).

The hull has a plate thickness of p = 4 mm. The lower base plate has a thickness of D_1 = 20 mm and the upper plate has a thickness of D_2 = 10 mm. The upper plate is indeed a ring, but is modeled in the FEM calculations as a full disc. The model also has three stiffening rings in the heights of h_1 = 1500 mm, 2500 mm and h_2 = h_3 = 2800 mm. These have a base height of s_1 = 155 mm and a web thickness of s_2 = 6mm. The profile of the reinforcing rings have a width of p_1 = 30 mm and a thickness of p_2 = 4mm.

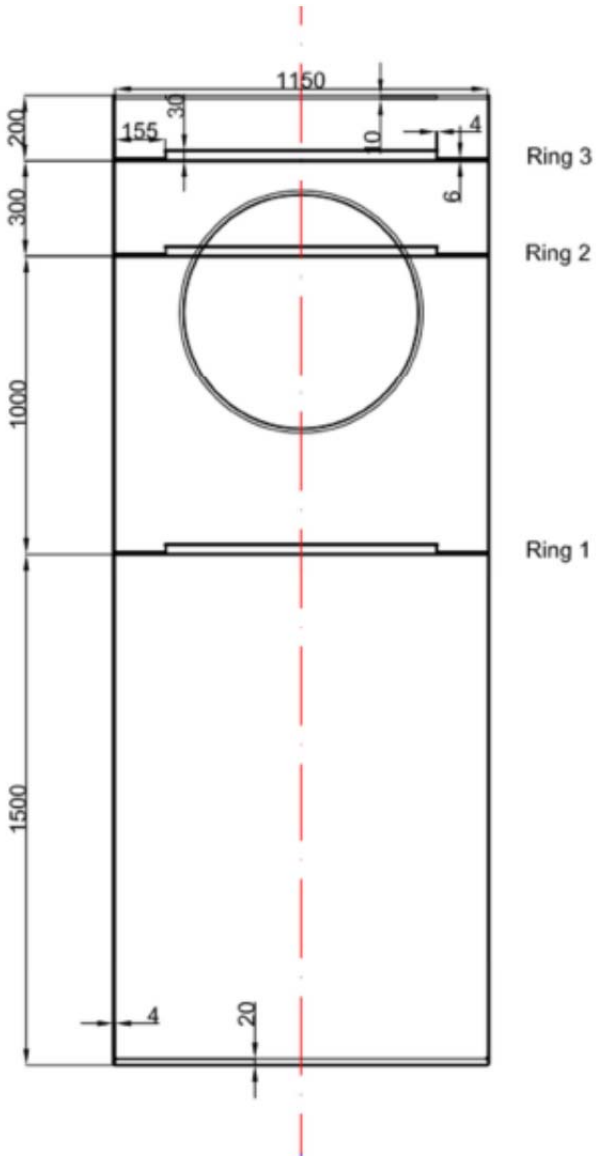

Figure 1 Main dimensions of existing cylinder

With the FEM model, two cases were studied. In the first case it is assumed that a circular symmetrical distributed ice pressure is acting on the cylinder [Case A] (see Figure 2).

In the second case, it is assumed that a cosinusoidal distributed ice pressure is acting on the cylinder [Case B] (Figure 4).

Case A

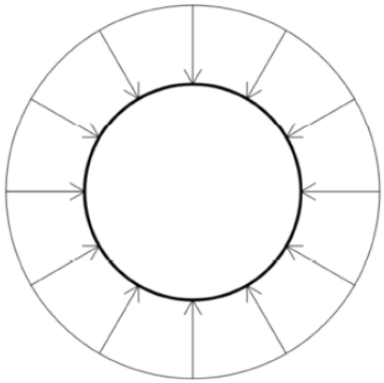

Figure 2 Schematic diagram showing symmetrical pressure distribution on cylinder

The distribution is described by the following function:

$$p(x) = p_0 \times cos\left(\frac{x\pi}{2R}\right)$$

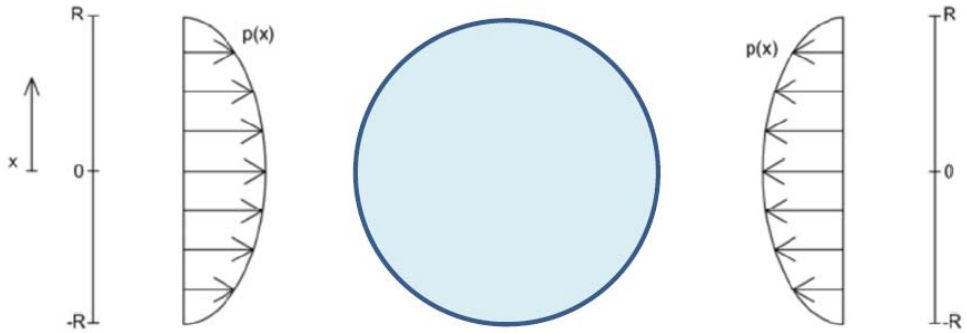

Figure 3 Schematic diagram showing cosine pressure distribution on cylinder

3.2 Results of FEM calculations

In order to describe the stress state of the cylinder, the stresses were evaluated according to the *von Mises* equivalent stress.

Case A

In this case (circular symmetrical ice pressure) the yield strength of σ = 235 N mm^{-2} is achieved at a pressure of 1.388 MPa. This stress occurs on the inside of the hull in close to the bottom (see Figure 4).

Figure 5 illustrates the deformations at a pressure of 1.388 MPa in the radial direction.

In both images, the deformations are scaled by a factor of 100.

Case B

In this load case (cosine ice pressure distribution) the yield strength of

σ = 235 Nmm^{-2} was achieved at a pressure of 0.1 MPa, This stress occurred at the inner edge of the first reinforcing ring at height h_1 = 1500mm

(see Figure 6).

.

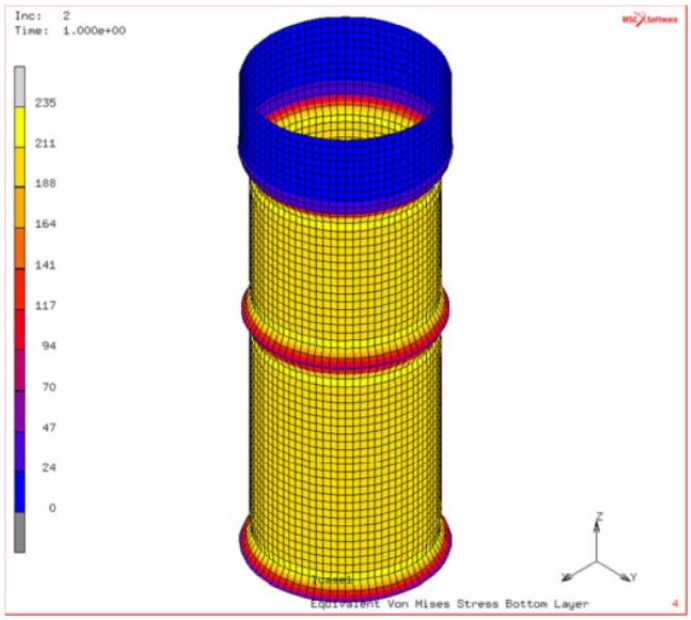

Figure 4 Distribution of *von Mises* equivalent stresses (Nmm^{-2}) on inner face of the cylinder (Case A)

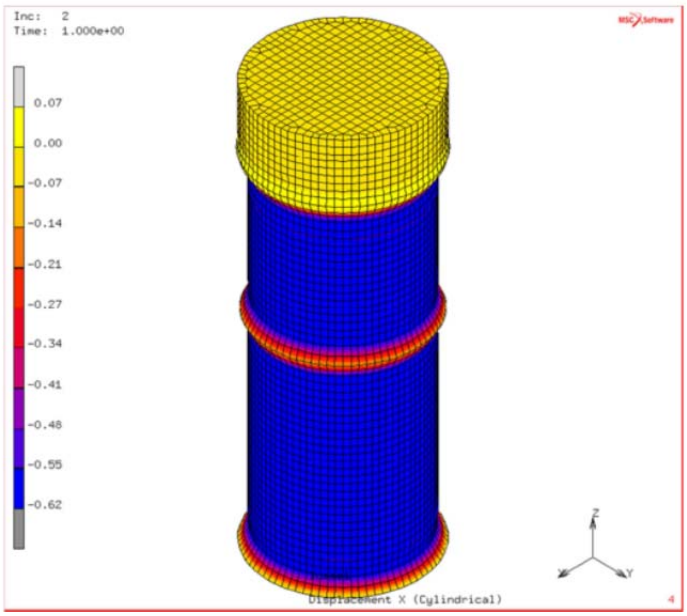

Figure 5 Displacement (mm) in radial direction on cylinder (Case A)

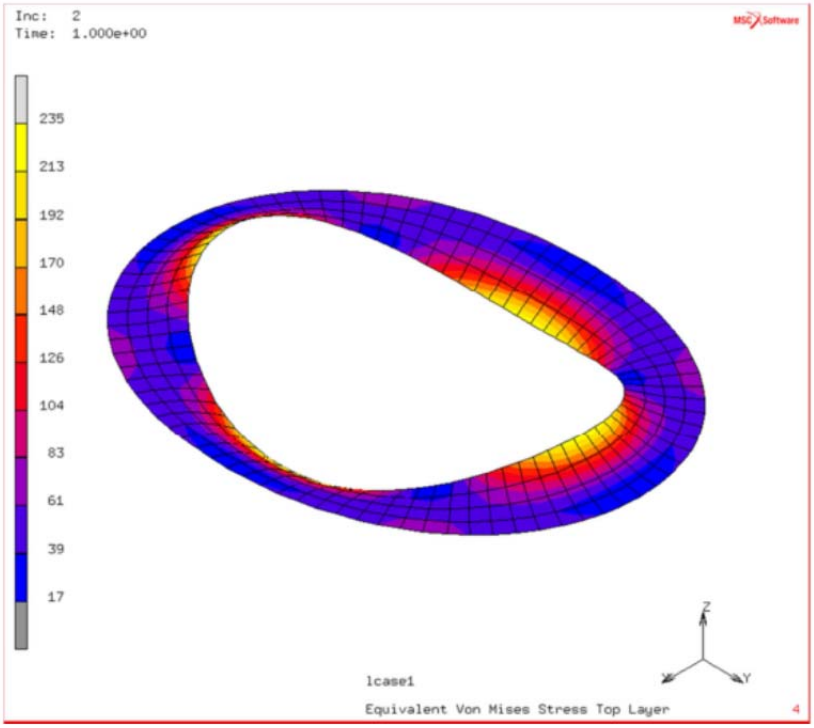

Figure 6 Distribution of *von Mises* equivalent stress (Nmm^{-2}) in stiffening ring (#1) of the cylinder (Case B)

The following figures show the *von Mises* equivalent stresses (Figure 7) and the radial deformation (Figure 8) of the cylinder. It is observed that the reference stress is low and the radial deformation is relatively large.

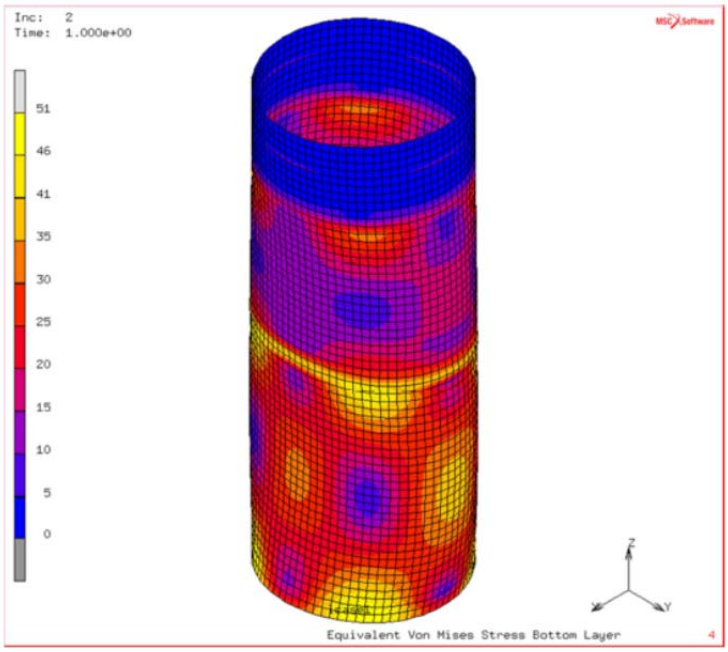

Figure 7 Distribution of *von Mises* equivalent stress (Nmm^{-2}) on outer face of the cylinder (Case B)

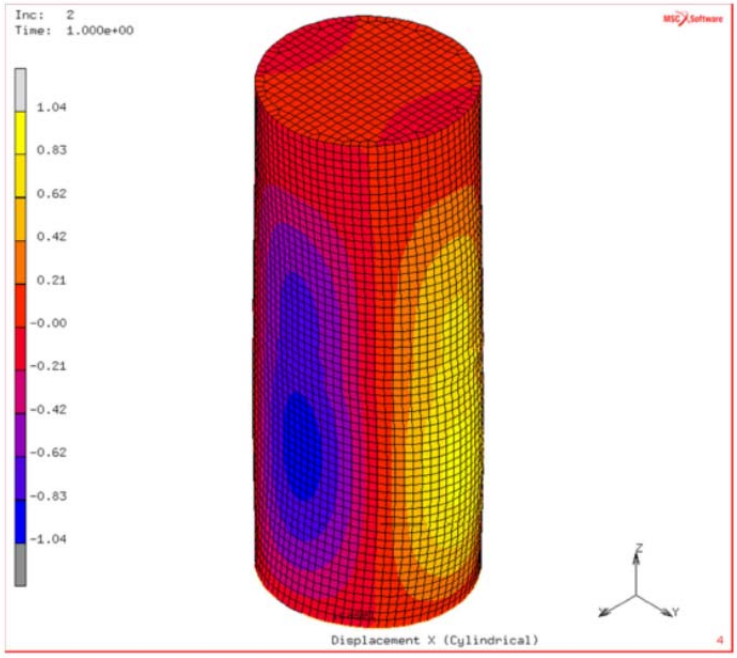

Figure 8 Displacement (mm) in radial direction on cylinder (Case B)

The results of the FEM calculation can be summarized as:

- The type of steel of the existing cylinder is subject to brittle fracture at low temperatures.

- For Case B the cylinder would deform elastically only up to a pressure of 0.1 MPa (100 kPa). If the pressure exceeds this value - what probably may happen in Arctic sea ice - it would result in permanent plastic deformation, which is not acceptable.

During the design phase of the LSB, it became evident that the production of the measurement system is too expensive. Due to the high weight of the LSB, problems regarding transportation, handling and insertion into the ice, high costs were expected. It was also recognized that timely completion could not be guaranteed. For these reasons, it was decided in consultation with the leader of WP 2, not to pursue the development of this measurement system and to search for an alternative.

4 Ice Camp in the Beaufort Sea

4.1 Data gathering strategy

Too little is known about temporal and spatial evolution of the ice pressure field, and the forces involved in deformation events in the Arctic. Under winter conditions sea ice has two main sources of stress, (1) changes in the ice temperature (thermal) and (2) changes in ice motion (dynamic). Thermally induced ice stresses are low frequency (order of days), while ice motion induced stresses have both a high-frequency (order of hours) as well as a low frequency components (Richter-Menge and Elder, 1998). Understanding and removing the thermal influence on the development of the strain and stress field within sea ice is a notoriously difficult process, especially within drifting ice. Drifting ice pack has the further complexity

that it is of variable thickness; thick ice is formed through ridge building processes and thin ice formed through the refreezing of leads.

To determine the role of ice dynamics in the evolution of pressure field our strategy is to install our stress buoy in the centre of a 5-ice buoy array (Figure 9). Therefore any differential movement observed by the buoy array should be reflected in the pressure measurements made by the stress buoy. Additional measurements of environmental parameters, such as ice temperature, wind and current field etc. were carried out.

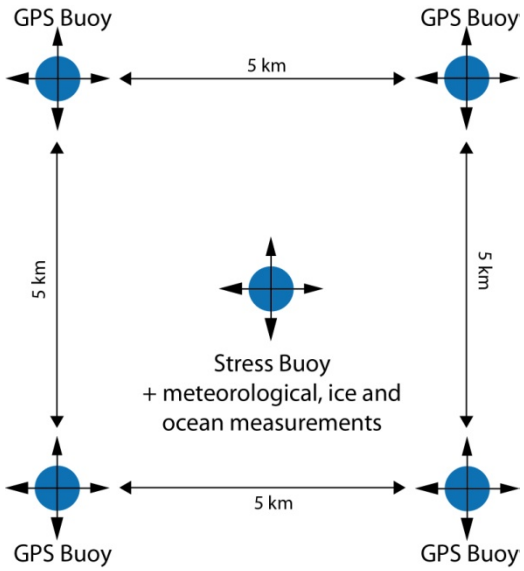

Figure 9 Schematic diagram of the deployment set up. Differential movements of the buoys should be reflected in the observed stress measurements.

We are extremely fortunate that we were able to take advantage of an **O**ffice of **N**aval **R**esearch **M**arginal **I**ce **Z**one (ONR-MIZ) programme that aimed to better understand the processes behind the recent retreat of Arctic sea ice. More information on this programme can be found here:

http://www.apl.washington.edu/project/project.php?id=miz

As a result we were able to take advantage of both the logistics and science that was being performed within this programme.

4.2 Field campaign

The opportunity to deploy the stress sensor buoy came through an ONR-MIZ programme. This programme had a dedicated spring field programme in March/April 2014. This time of year was perfect for the deployment of our Stress buoy, as the days are getting longer but the snow and sea ice is still cold.

The timing window for safe and efficient fixed-wing aircraft on-ice support indicates that all fieldwork should be completed prior to mid-April. Between March and mid-April the weather is generally good, and thus it is advantageous for aircraft and on-ice operations. After this time the environmental conditions degrade i.e. fog is more common, and the melting of snow/sea ice makes for unsafe landing conditions.

To ensure that the full spatial and temporal evolution of the seasonal sea ice cover is monitored continuously by the MIZ programme the instrument deployment area covered a 300 km swath of the Arctic Ocean. This deployment region was situated in the Arctic Ocean proper, a couple of hundred kilometres from Banks Island, Canada. The deployment line ran in a N – S direction from latitude 72° to 75° N and was situated in the 135° W longitude line.

4.2.1 Logistics Base

Given the deployment location was near Banks Island, we used Sachs Harbour (71.9856° N, 125.2481° W) as our logistic base for our operations. It is from here that we mobilised our on-ice deployment operations. Our Stress Buoy was transported (with the rest of the MIZ equipment) to Sachs Harbour via a chartered Hercules aircraft. From Sachs Harbour our Stress buoy was flown out to Camp 2 via a Twin Otter flight.

The schematic in Figure 10 shows the location of Ice Camps in relation to Sachs Harbour, Banks Island and the deployment shape of the MIZ autonomous platforms. The IDEAL Ice Force Panels were deployed at Camp 2.

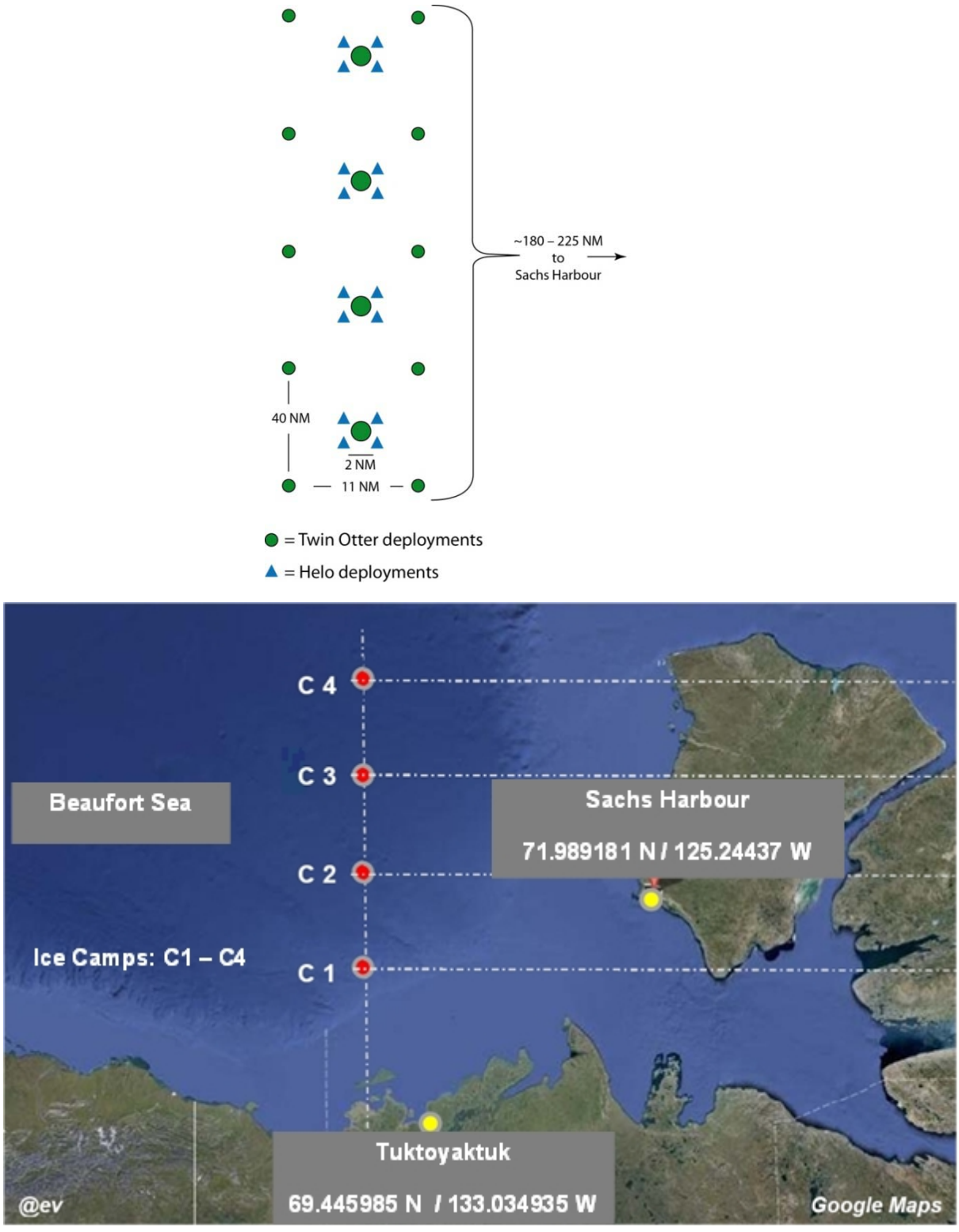

Figure 10 Location of Ice Camps C1 to C4 in relation to Sachs Harbour, Banks Island.and Tuktoyaktuk, NWT

4.2.2 Aircraft operations

A number of different aircraft were utilised by the programme. These were:

1) Commercial High Capacity Cargo:
    a. First Air Hercules aircraft were used to move all the equipment, supplies, and fuel from Yellowknife (Can) to Sachs Harbour (Can). Including the stress buoy and its associated electronics

2) Kenn Borek/Aklak Twin Otter:
    a. For transport of equipment, fuel and personnel as well as runway scouting.

3) BAS Twin Otter:
    a. For transport of equipment, fuel and personnel as well possible science missions.

4) Helicopter (Great Slave Helicopters):
    a. The Bell 412 helicopter was used to deploy instrumentation from the centre of an array to the corners of each array.

4.2.3 Ice camps

A total of four mini ice camps were set up during the MIZ operations. These were numbered from one to four, with the most southerly camp being number one and the most northerly being numbered four. Ice runways were established at all four sites. Base camps were established at C2 and C3, and warming tents at C1 and C4. All non-scientific equipment was removed and backhauled to Sachs Harbour. The stress buoy was deployed at Camp 2.

Figure 11 Ice camp with the two twin-otter aircraft and helicopter

4.2.4 Bear Safety

Our project abided by Canadian laws with respect to bear safety (i.e., hunting

regulations) and firearms laws. Air horns and marine signal flares were provided as the first line of bear deterrence. When on the ice we also hired Inuit hunters from the Sachs Harbour Hunters and Trappers Committee as bear guards. Shotguns were available at each camp (C2, C3), and for personnel working at remote sites (C1, C4).

4.2.5 Methodology

We were particularly fortuitous as the position/shape of the 5-dice array needed to fulfil our goals, were identical to the needs of the ONR deployment strategy for their instrumentation. The distance between the outer buoys in array was about 5 km. At each outer leg of the array an Ice Mass Balance Buoy (IMB) and a Wave Buoy (WB) was deployed. In the central region of the array, where the stress buoy was situated, there was an additional Ice Mass Balance Buoy and a Wave Buoy as well as an Automatic Weather Station (AWS), Ice Tethered Profiler (ITP) and and Arctic Ocean Flux Buoy (AOFB). It is the IMB and AWS data that we are most interested in, but the GPS data from all buoys will provide information on the ice dynamics, whilst data from the ITP and AOOB provides information on upper ocean currents and properties.

An example of the ice conditions (with IMBs and WBs in photo) at deployment of one of the ONR clusters can be seen in Figure 12.

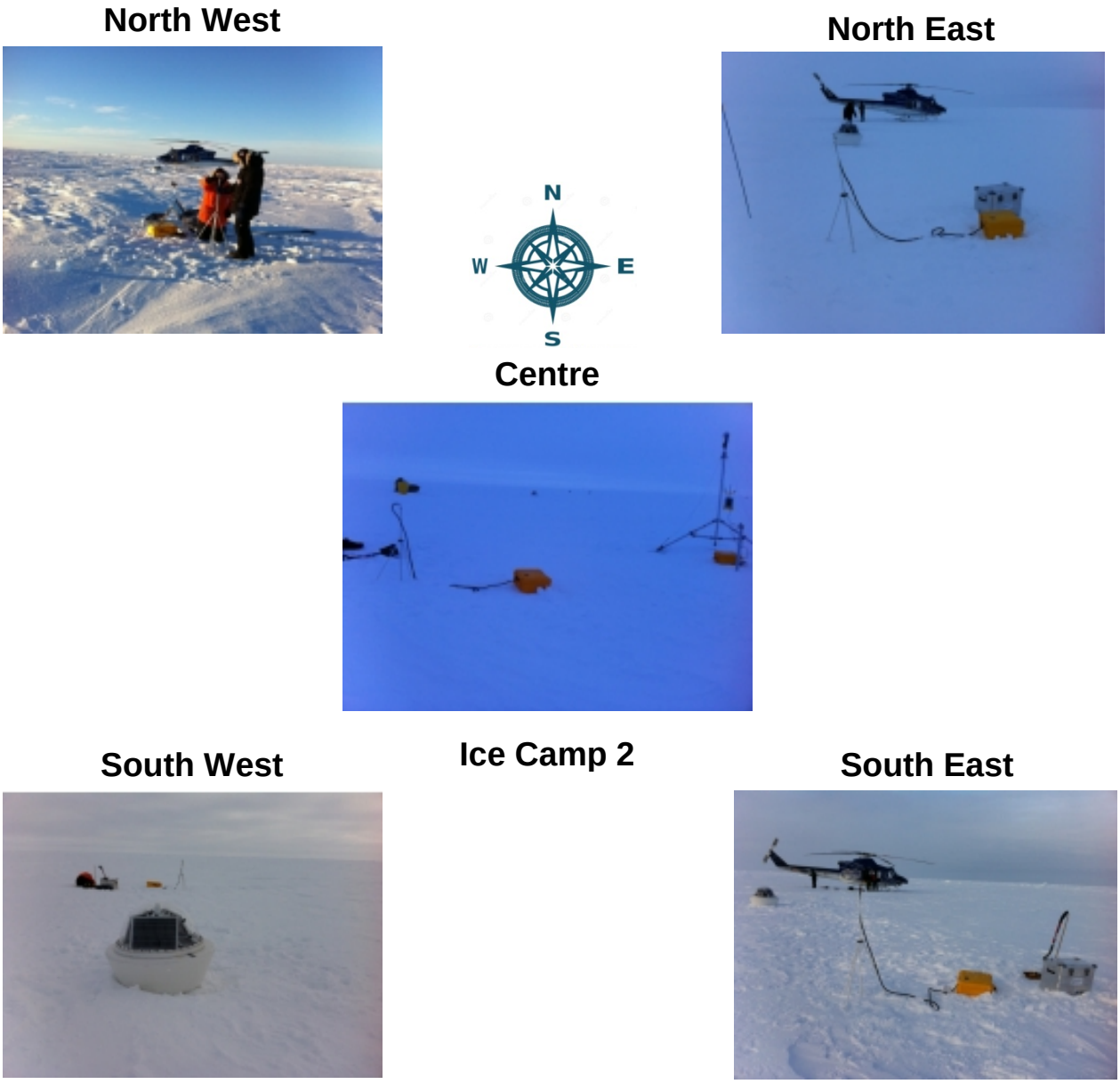

Figure 12 Ice conditions at Camp 2. In the photos the IMBs can be seen (yellow box) and the WB can be seen in the centre photo. The separation of the outer arms of the array is about 5 km.

4.2.6 IDEAL™ Ice Force Panel System (IFP)

The Stress buoy is built around the IDEAL ™ Ice Force Panel (IFP) system, which was supplied by Terrascience Systems Ltd, Canada. Each panel is divided into four

subsections and is designed to measure up to 2 MPa of normal stress.

The IFP consists of a three 0.5m x 0.5m panels wired to a central data acquisition unit (DAU). In order to understand/compensate the effect of temperature on the DAU and IFPs two thermocouples are connected to the DAU.

The DAU uses a standard SD card for data storage. Data is retrieved via an on-board Ethernet port (see Figure 13). The system is fully autonomous as solar panels linked to two 12 volt batteries keep the system running continuously without the need for human intervention.

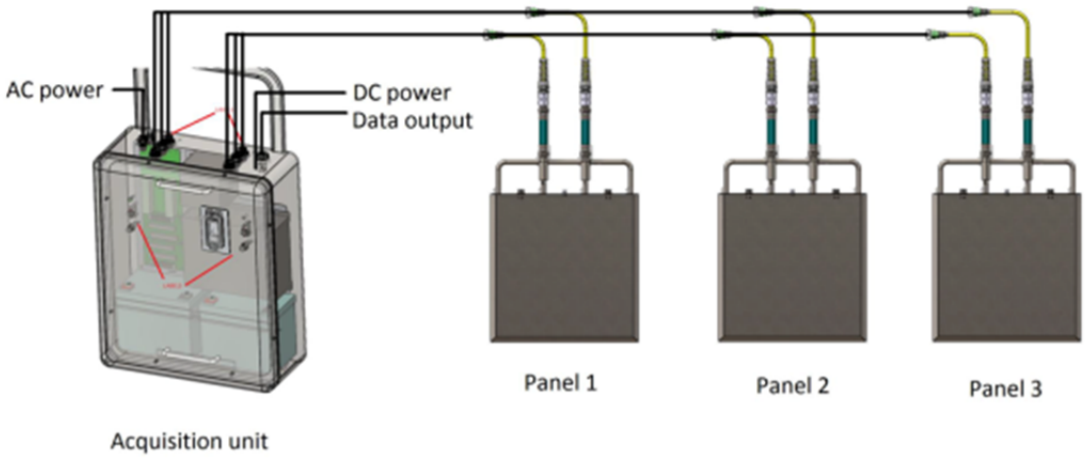

Figure 13 Basic set up of the data acquisition unit, solar panels and shunt regulator not shown (schematic courtesy of Terrascience Systems Ltd, Canada).

4.2.6.1 Calibration of panels

Each IFPs has a direct linear relationship (1:1) between load and output. However the relationship does vary slightly between and cells and panels, as such each of the four zones of each panel needs independent calibrating. The results of these calibrations can be seen in

Figure 14 - Figure 16.

Panel 1

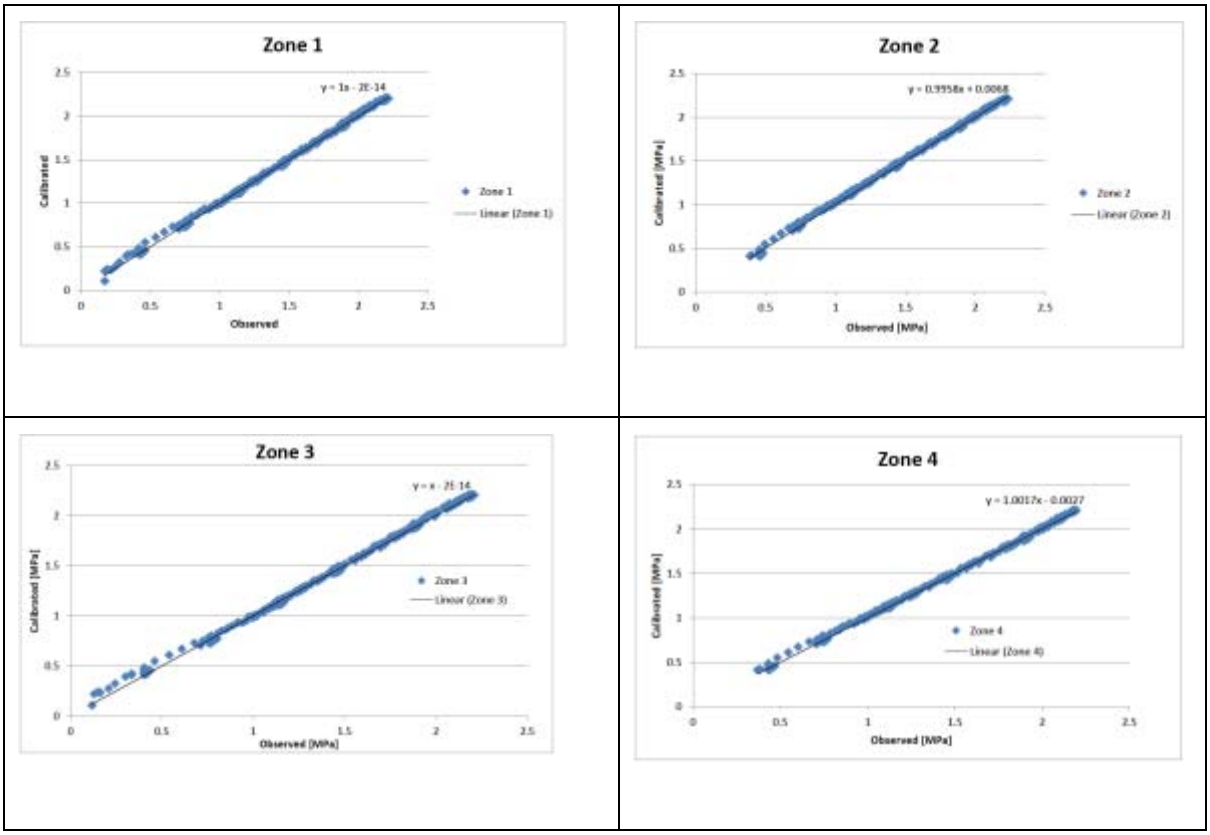

Figure 14 Plots of IFP (1) Calibration

Panel 2

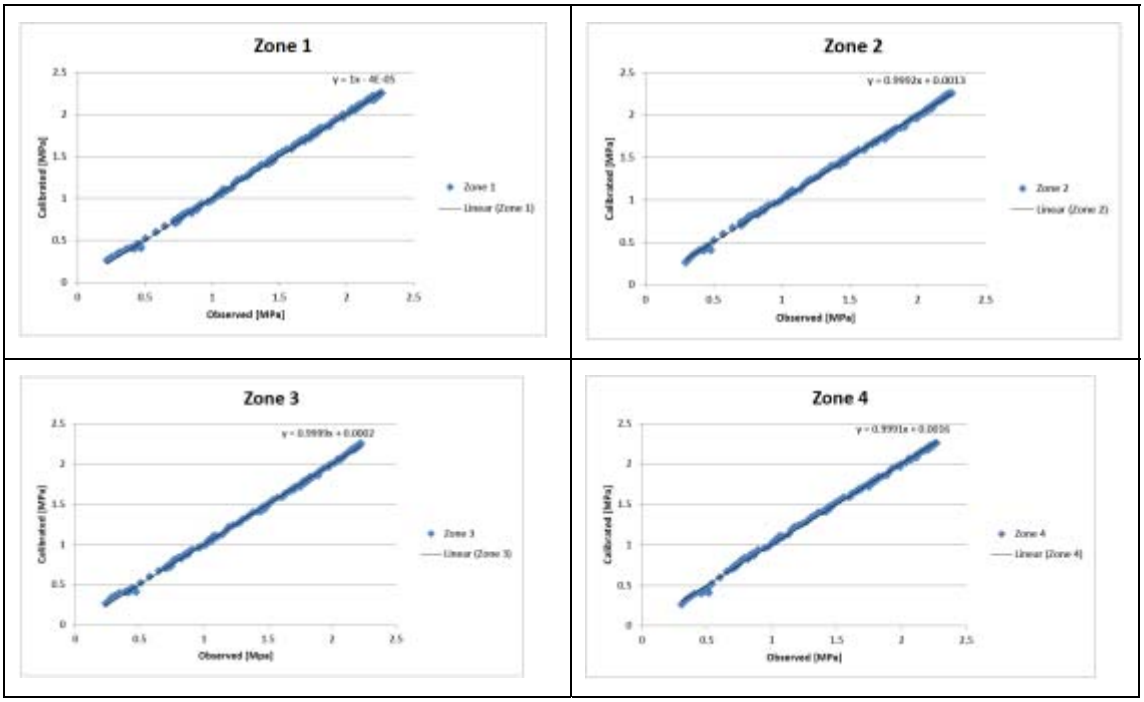

Figure 15 Plots of IFP (2) Calibration

Panel 3

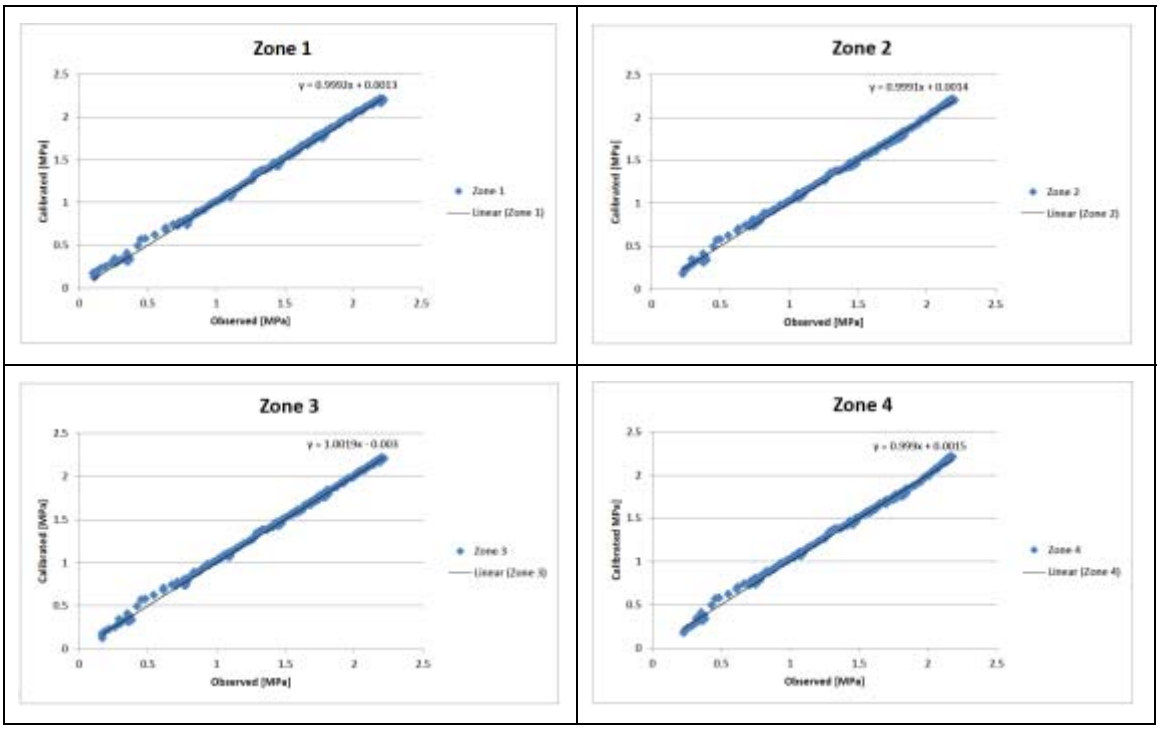

Figure 16 Plots of IFP (3) Calibration

4.2.6.2 Deployment of Panels

The deployment of the system is quite time consuming, especially within cold (hard) sea ice. An individual 0.5 x 0.5 m IDEAL^{TM}- Ice Force Panel is shown in Figure 17 and the fully integrated system deployed is shown in Figure 18.

.

The procedure was as follows:

1) shovel snow off the chosen site,

2) chisel out a three slots, at 120° to each other. The slots should be deep enough to completely cover each IFP panel.

3) place IFP panel in each slot. As each IFP is orientated at 120° to each other so that we can determine the direction of stress.

4) Flood slots with sea water. This was achieved by drilling hole through the bottom of the slot and into the ocean below.

5) Turn IFPs on

6) Slots freeze up and become one with the surrounding sea ice.

Figure 17 IDEAL^{TM}- Ice Force Panel (0.5 x 0.5 m)

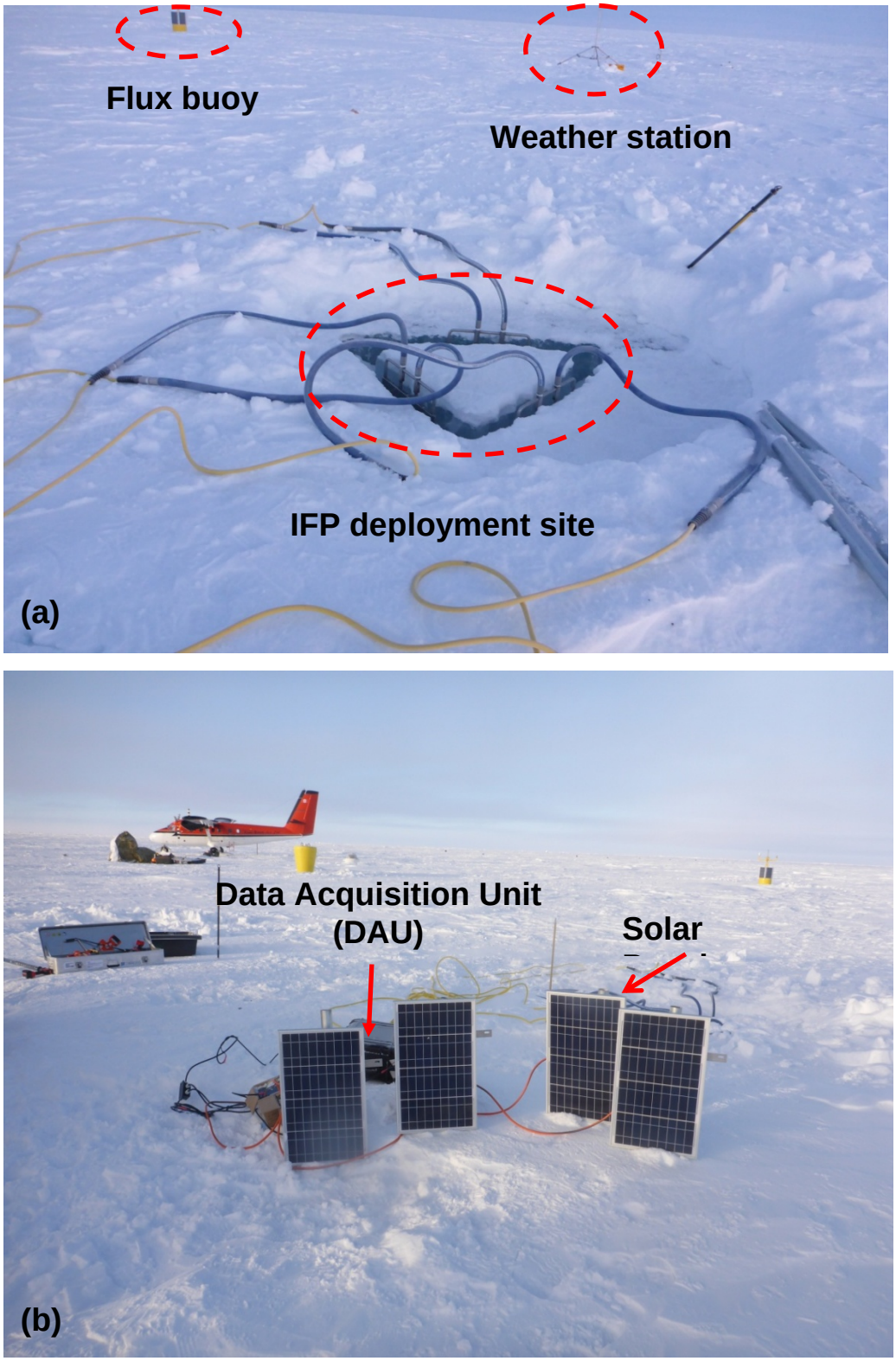

Figure 18 (a) Slots cut in the ice and IFPs deployed and (b) fully integrated system deployed

4.2.7 Ice mass balance (IMB)

Inference of ice growth or melt at the surface and bottom of the sea ice depends on accurate knowledge of the ice–ocean interface, which in the case of IMB buoys, relies on measurement of both the ambient temperature and the thermal response of the immediate surroundings of the heater/sensor pairs to short periods of heating. The thermal response of air, snow, ice, and water to this heating cycle is different, and thus the medium the sensor is embedded in can be recognized. Once the interfaces have been identified the rate of change in the position of the interface along the chain is interpreted as the melt or growth rate.

Generally an IMB chain is 5 m long with temperature sensors spaced at 2 cm along its length. This allows a portion of the chain to sample the ambient air, snow, ice, and upper water column temperature (see Figure 19).

The ice thickness data along with the temperature profile and GPS data from can be used to help understand the internal stress field within the ice. For more details about the IMB see WP1, Task 1.2.2 Monitoring snow, sea ice thermodynamics and sea ice drift.

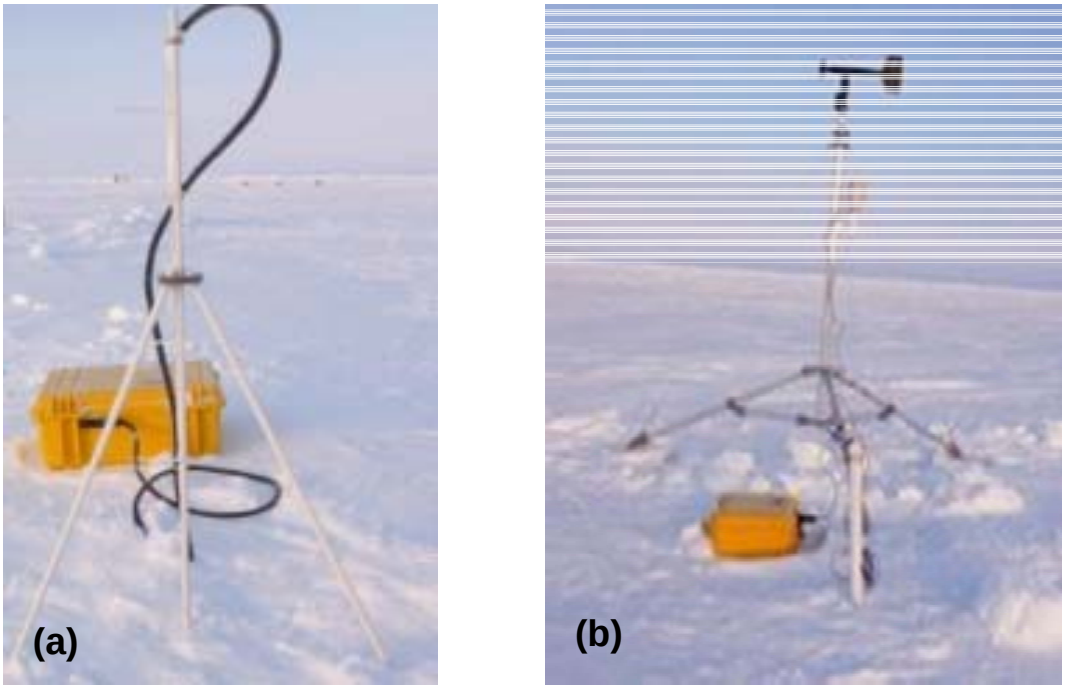

Figure 19 Ice Mass Balance buoy (IMB) Automatic Weather Station (AWS) from BAS

Results

A fault in the internal SD card-holder of IFP data acquisition unit meant that no data was recorded during the Ice Camp field campaign.

This is particularly disappointing because on the one hand it was possible to design and produce the ice stress measurement system and on the other hand, all constructive, technical, and logistical preparations were carried out for this Ice Camp campaign with huge effort to investigate the lateral pressure in Arctic sea ice.

Because there is still too little information about the lateral ice pressure, it is necessary to perform interdisciplinary field campaigns with geophysicists, meteorologists, oceanographers and ice engineers in the Arctic in the future.

In such a campaign a better understanding of the lateral pressure of the ice can be obtained by use of complementary data sets.

An example of the meteorological data for the month of March and April 2014 in the Beaufort Sea can be seen in Figure 20.

Due to the fact that the measurements of the lateral ice pressure have not been successful, a literature review is carried out in Section 5.

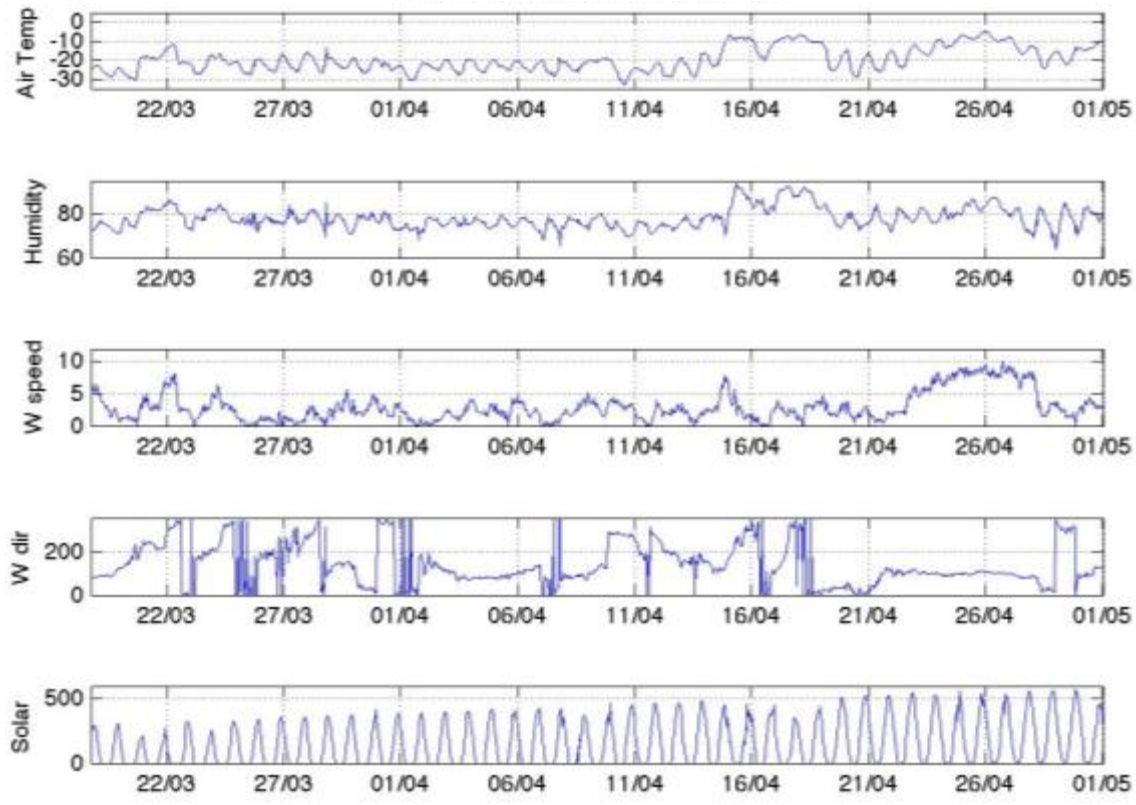

Figure 20 Meteorological data from AWS during March and April 2014.

5 Literature review: Stress measurements in sea ice

This section is focussing on a literature review about stress measurements in sea ice.

5.1 Sea Ice Mechanics Initiative (SIMI) in the Alaskan Beaufort Sea (Winter 1993/94)

A field program Sea Ice Mechanics Initiative (SIMI), to monitor ice stresses in sea ice was carried out in the Alaskan Beaufort Sea. During a 6 month period in the fall-winter-spring of 1993-94 stresses were measured on different sites of a multi-year ice floe embedded in pack ice.

The camp site was a multiyear floe approximately 450 km north of the Alaskan coast (75°N, 142°W) as shown in Figure 21.

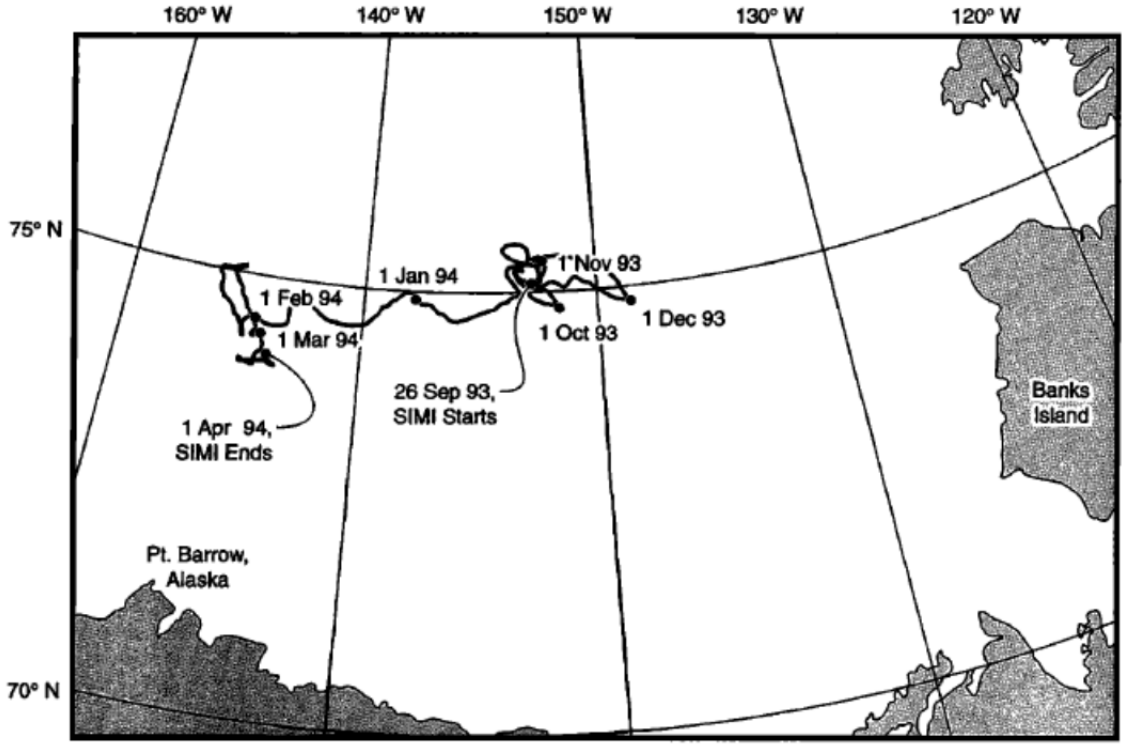

Figure 21 Drift track of the multiyear floe that served as a base camp for the Sea Ice Mechanics Initiative (SIMI), (*Richter-Menge and Elder, 1998*)

The multi-year floe was roughly 2 km in diameter and had an average ice thickness of 1.44 m in mid-November 1993.

At the end of field campaign in early April 1994, the floe had drifted approximately 250 km to the west (74°N, 155°W). As shown in Figure 21, most of this movement occurred during December and January. The total rotation of the floe over the course of the experiment was estimated to be 60°, clockwise.

In the period December through March the camp was not occupied, however the equipment installed on the floe was designed to run autonomously and data were collected without interruption through the entire experiment.

5.1.1 Stress sensor type used during SIMI program

For the in situ measurements cylindrical vibrating wire sensors described by Johnson and Cox (1982), Cox and Johnson (1983) were applied. These sensors have undergone extensive laboratory tests to determine their reliability (Cox and Johnson, 1983) and have been successfully used in other Arctic field programs (Johnson et al., 1985; Tucker and Perovich,1992).

The sensor gives information on the stress acting at a point in the horizontal plane of the ice cover. Stresses are determined by measuring changes in the radial deformation of a cylindrical steel annulus, using a 120°, three-wire rosette. The wires in the rosette stretch across the hollow center of the annulus at the mid point along its length. Changes in the diameter of the annulus cause a change in the frequency of vibration of each wire, which are plucked magnetically. Knowing the material properties of the steel annulus, this change in frequency can be directly related to the stress applied to the sensor (Cox and Johnson, 1983).

5.1.2 Sensor deployment

A total of seven sensors were deployed in the multi-year ice floe at each of the edge sites. Five of these sensors were positioned along a line that extended from the edge to the center of the floe. They were located at 2, 5, 10, 25, and 75 m from the edge. Between the measurement sites the major principal compressive stress components varied significantly. Stresses of greater magnitude and more high frequency variations were measured at the ice edge than at the center of the ice floe. At a distance of about 400 m from the edge of the floe, maximum stresses ranging from 100 to 300 kPa were measured (*Richter-Menge and Elder, 1998*).

All of the sensors were placed near the surface of the ice, an average of 22.1 cm below the ice surface with the exception of the site at the center of the floe where sensors were also located at depths of 1.0 and 2.0 m (*Richter-Menge and Elder, 1998*). In total 137 thickness measurements were conducted in the floe during the survey. The mean ice thickness was 1.44 ± 0.85 m, with a range of 0.39 to >4.00 m (

Figure 22).

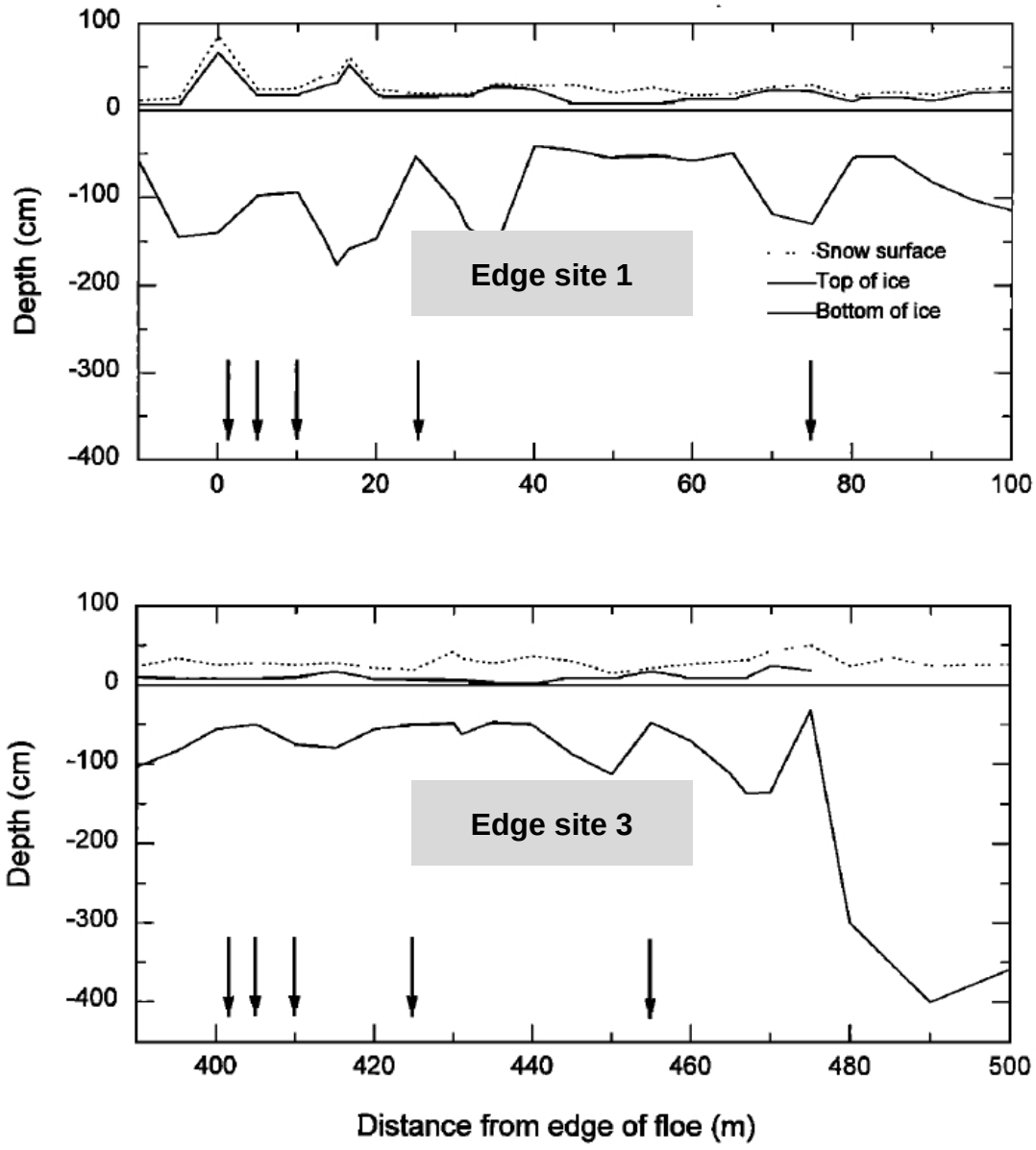

Figure 22 Ice and snow thickness distribution at stress sensor edge sites located near the edge of the multi-year floe. Arrows indicate the location of the stress sensors (after R*ichter-Menge and Elder, 1998*)

5.1.3 Results

The time series for major (σ_1) and minor (σ_2) principal stresses measured at edge sites 1 and 3 and center site are presented in Figure 23.

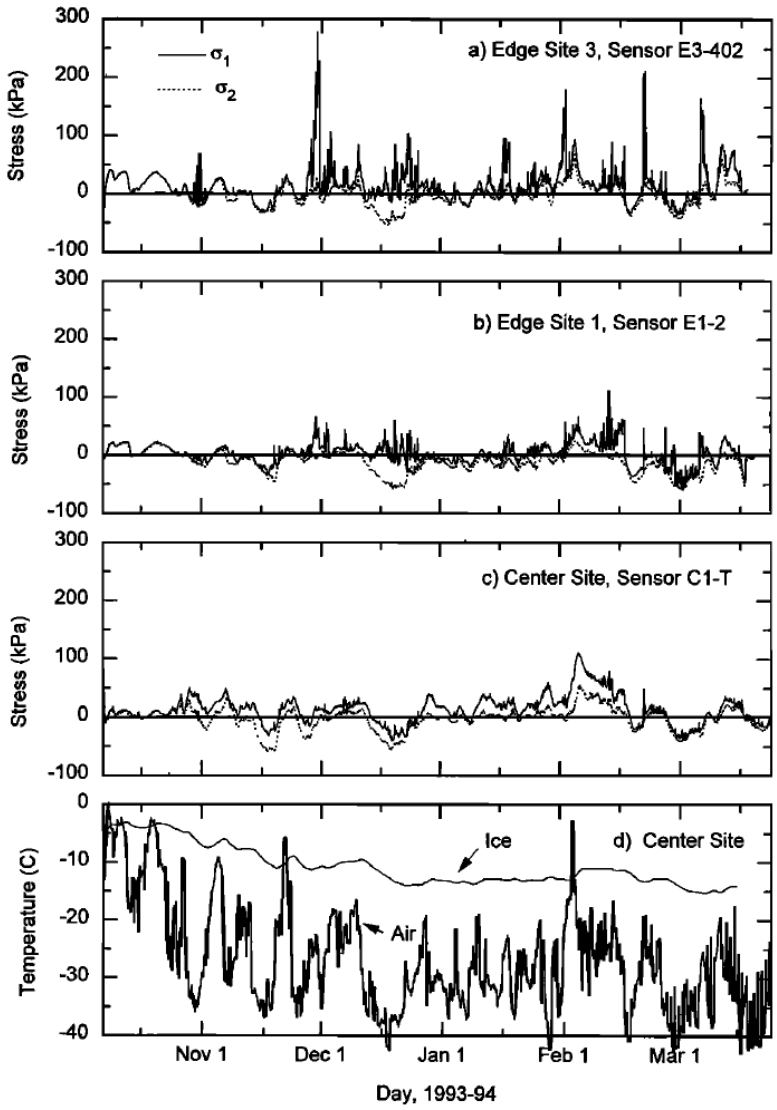

Figure 23 Time histories of the major σ_1 and minor σ_2 principal stress components at (a) edge site 3, (b) edge site 1, and (c) center site, and (d) the ice and air temperature at the center site, from October 7, 1993 to March 21, 1994.

At edge site 1 the sensor was 2 m from the edge, and at edge site 3 it was 400 m from the edge. All three records give near-surface stresses. The depths below the ice surface of the wire rosette in the sensors at center site, edge site 1, and edge site 3 were 0.38, 0.44, and 0.20 m, respectively.

Because of the strong correlation between the ice temperature and the minor principal stress an approach for separating the thermal and ice-motion-induced stresses. If the minor principal stress is primarily a function of changes in the ice temperature and thermal stresses are isotropic in the plane of the ice cover, then the ice-motion-induced stresses can be estimated by subtracting the minor from the major stress (Richter-Menge and Elder, 1998). The results are presented in Figure 24.

Under certain loading conditions ice-motion-induced stresses may, in fact, be predominantly compressive. However, even in these cases, irregularities in the thickness of the multi-year floe are likely to cause bending, which can result in tensile stresses (Hallam et al., 1989; Frederking and Evgin, 1990; Sukhorukov, 1995). The estimated ice-motion-induced stress exhibits both high- and low-frequency variations at all of the sites. There are no significant changes in the relative magnitude of the peak stresses nor in the relative distribution between the sites for the estimated ice-motion-induced stress. Edge site 3 still shows more pronounced high-frequency activity than edge site 1, and center site remains dominated by low-frequency variations. The difference between characteristics of the estimated ice-motion induced stress between the edge and center sites may reflect the complex process of stress transmission through floe and, more generally, the ice pack (Richter-Menge and Elder, 1989).

.

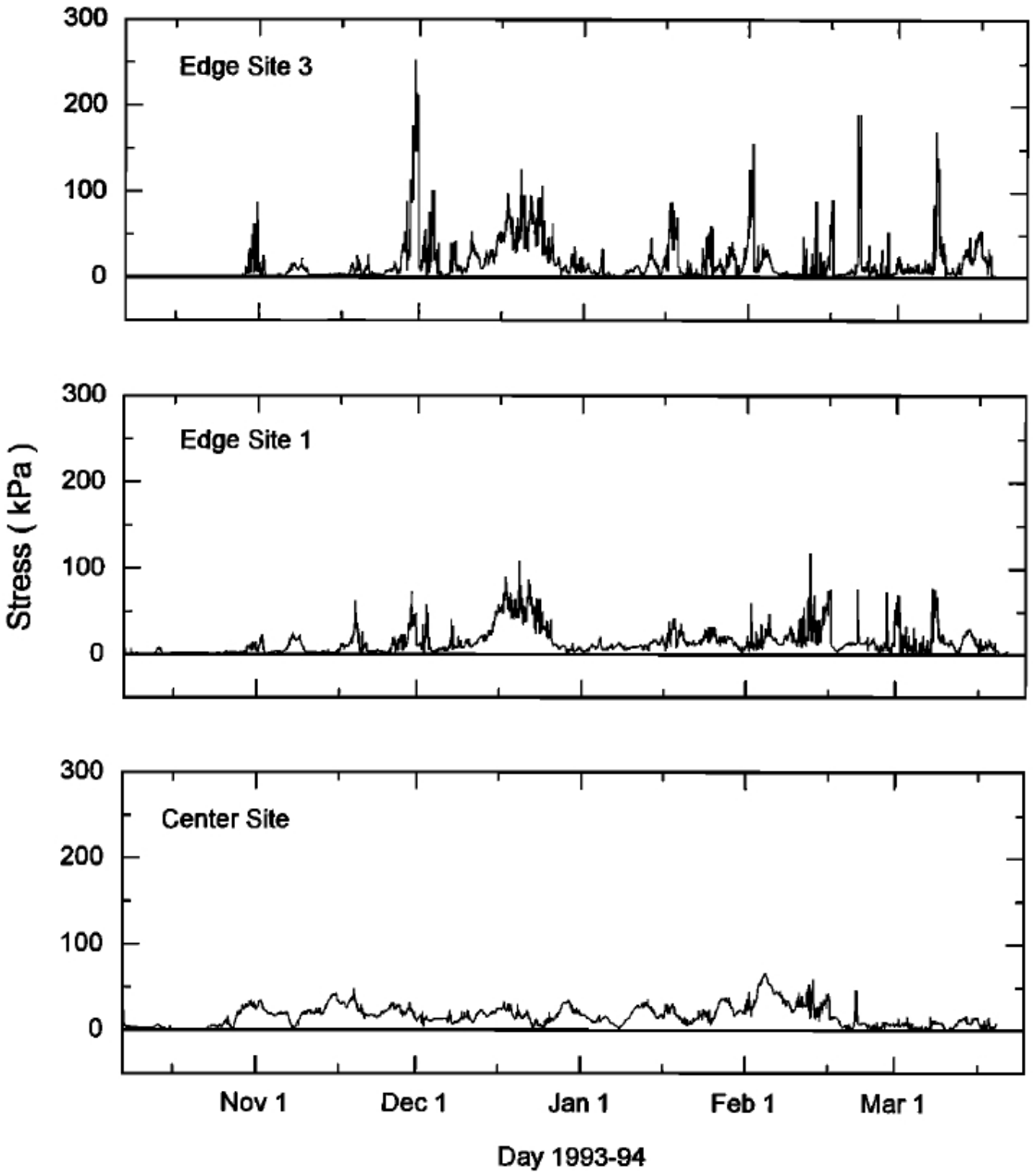

Figure 24 Estimated ice-motion-induced stresses obtained by subtracting the minor from the major principal stress component (*Richter-Menge and Elder, 1998*)

Ice-motion-induced stresses occur in response to wind and current forcing and can result in the formation of ridges, leads, and rubble fields. Observations of stress and ice deformation have shown that these ice deformation events are associated with

large and rapid changes in the ice stress (*Johnson et al., 1985; Coon et al., 1989; Comfort et al., 1992; Tucker and Perovich; 1992*).

Similar observations during this field campaign were made. In two cases, November 29 and February 17, visual inspections of the floe before and after these events indicate that rapid decrease in stress was associated with cracks and, subsequently leads forming across the multi-year floe. Nobody was on the floe to make similar observations during other periods of significant stress activity.

The results obtained from this field campaign can be summarized as:

- The magnitude of the thermal stresses is relatively constant at a given depth over the extent of a multiyear floe.
- Ice-motion-induced stresses, which in the winter are primarily caused by atmospheric forcing, exhibit significant spatial variability over the extent of a floe.
- At the edges of a floe, ice-motion-induced stresses are most easily distinguished by rapid variations in magnitude, which occur at a frequency of the order of hours.
- The magnitude of the combined thermal and ice-motion induced stresses displays significant temporal and spatial variability in compression. Maximum compressive stress, measured at a site 400 m from the edge of the floe, typically ranged from 100 to 200 kPa and suggests a ridge-building force of the order of 150kN m^{-1}.
- These stresses are significantly attenuated as they are transmitted from the edge to the center of the floe.
- Tensile stresses are much more consistent over the entire floe, reaching a maximum of 50 kPa. The relative magnitude of the stress between sites at the edge of the floe, the direction of the principal stress, and a correspondence in the time of occurrence of episodes of significant stress activity between the sites remained fairly constant during the experiment.
- There are seasonal changes in the characteristics of the total stress. Thermally induced stresses are dominant in the fall.
- Ice-motion-induced stresses become more persistent as the winter season progresses. This suggests that the ice cover cannot effectively transmit

stresses through the pack until the new ice that develops in the fall between the multiyear floes becomes thick and rigid enough to create a mechanical continuum.

- Together, these results demonstrate the complex process of stress transmission specifically through a multiyear floe and more generally through the ice pack. A more detailed understanding of the process of stress transmission through the floe can be developed (*Frederking and Evgin ,1990*), i.e. a finite element model (FEM) can be used to estimate the boundary conditions that produced the stress distribution in the floe.

5.2 Surface Heat Budget of the Arctic Ocean (SHEBA) field experiment

During the SHEBA field experiment (winter 1997/98) sensors to measure the internal ice stress at several locations within a 15 x 15 km area were deployed on a drifting multi-year ice floe (Figure 25). The objective of SHEBA experiment was to collect data and to make these data sources available for evaluating sea ice dynamics models by assessing whether the stress signal can be qualitatively linked to the regional-scale (10–100 km) deformation activity (*Richter-Menge et al., 2002*). Stress sensors were used to make direct measurements of the internal ice stress. Satellite coverage of the ice conditions during SHEBA experiment was extensive. Therefore, satellite-derived ice motion products were used to assess the corresponding regional ice deformation.

Richter-Menge et al. (2002) report about 4 case studies, each with distinguishing characteristics:

a) consolidation of the seasonal ice zone against the Alaskan coast (5–7 December 1997)

b) advancement of the consolidation zone into the perennial ice pack (11–13 December 1997)

c) extreme divergence (14–17 January 1998); and consolidation of the pack against Wrangel Island and the Siberian coast (20–23 February 1998)

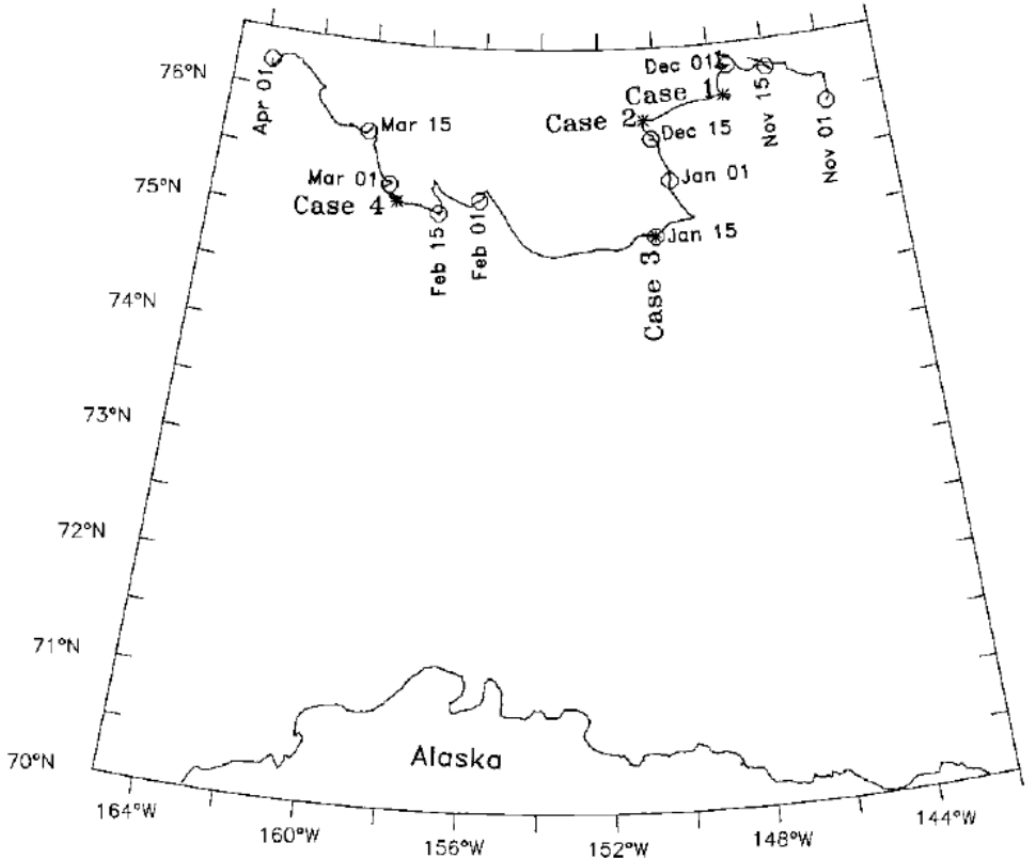

Figure 25 Track of drifting Ice Station SHEBA (*Richter-Menge et al. 2002*)

The results can be summarized as:

The results of this work give qualitative evidence of a relationship between internal ice stress measurements and ice deformation at the regional scale. During periods of ice convergence, the internal ice stress increases, and during periods of divergence, the internal ice stress decreases. This observation comes as no surprise; it reflects basic material properties and has been used as a fundamental element in the successful development of numerous sea ice dynamics models. The novel component to this work is a demonstration of the ability to observe this material behavior with direct measurements of internal ice stress and deformation.

The direct measurements provide insight into the process of regional ice deformation. It becomes clear from the examples we have presented that the

relationship between the internal ice stress and deformation is complex because of the effects of the state of the ice cover, coastal boundaries, and forcing conditions. In general, internal ice stresses develop in the winter ice cover when:

1) the seasonal ice cover has completely developed between the perennial ice and the coast,

2) moderate to high winds occur over a sustained period, at least 2–3 days,

3) these winds drive the ice toward a coastal boundary.

Consistent with the behavior of a granular hardening plastic, the internal ice stress increases until the ice cover fails, resulting in the development of lead and ridge systems. The extent of the failure region depends on the duration of the forcing conditions.

After the ice in the seasonal ice zone is compacted against the shore, ice stress propagates away from shore, and shear deformation can occur throughout the seasonal ice zone (*Richter-Menge et al.,2002*)

For shear to occur through the seasonal ice zone and into the perennial ice zone, creating large fractures covering several hundreds of kilometers, there must be sustained wind-forcing conditions that last for several days to weeks. The event ends with a change in wind direction, and ice must adjust to the new prevailing conditions (*Richter-Menge et al.,2002*).

Measurements of the ice velocity indicate that between 19 and 25 January 1998, when the average internal ice stress was near zero (see Figure 26a), the average rate of ice movement was about 15 km per day, with a maximum of 35 km per day. For comparison, the average rate of ice drift from 1 November 1997 to 1 April 1998 was approximately 8 km per day.

Figure 26 shows time series of the (a) internal ice stress and the standard error of the mean (SEM), (b) surface wind speed and floe speed, and (c) wind direction and floe direction measured during SHEBA, from 1 November 1997 to 1 April 1998. The internal ice stress represents an average of the ice-motion-induced stress, estimated

from measurements at eight different sites. The wind speed was measured 2 m above the ice surface. Wind and ice motion data are derived from measurements taken by the SHEBA Project Office at Ice Station SHEBA. The shaded bands denote the periods of the case studies.

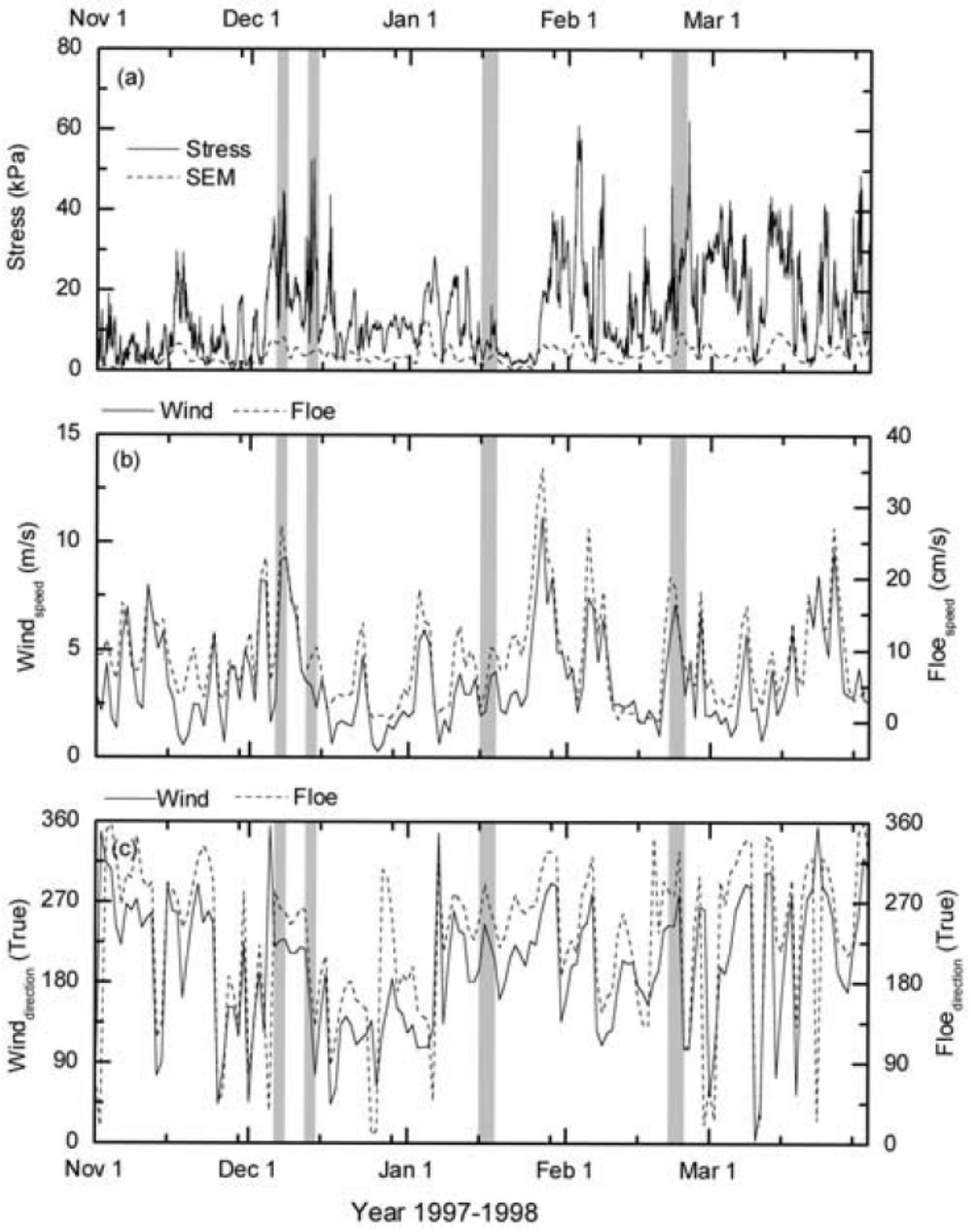

Figure 26 Time series of the (a) internal ice stress, (b) surface wind speed and floe speed, and (c) wind direction and floe direction (*Richter-Menge et al., 2002*)

A comparison of the stress time history between individual SHEBA sites showed that, in general, there was a strong temporal correspondence in the stress activity at the different sites. This suggests that all of the sites were reacting to the same loading event. However, the specific characteristics of the stress at the individual sites, including the relative magnitude and the time of peak activity, showed significant spatial variability. *Richter-Menge et al. (2002)* believe that the complex spatial variability reflects the influence of the ice thickness distribution, the dominant loading direction, and the proximity to local deformation activity.

Richter-Menge and Elder (1998) demonstrated, that, under winter conditions in the central Arctic, ice-motion-induced stresses can be estimated by subtracting the primary principal stress from the secondary principal stress (σ_1 - σ_2). This approach is based on the following observations:

1) ice-motion-induced stresses are highly directional,
2) changes in the ice temperature create stresses that are isotropic in the horizontal plane of the ice cover,
3) changes in the ice temperature are strongly correlated with the secondary principal stress.

5.3 Ice pressures at Adams Island (Lancaster Sound) in winter 1983/84

Field measurements of environmental conditions and ice cover responses were made around Adams Island in the Lancaster Sound area over the winter of 1983/1984.

A number of participants were involved in the project which has extended over three winter seasons. The National Research Council Canada (NRCC) coordinated the project and was involved in measurement of movements and large-scale deformations of the ice - cover, as well as in characterization of ice behaviour. The Atmospheric Environment Service (AES) was involved with the measurement of air temperature, wind, and drag, and the Department of Fisheries and Oceans, with measurement of current and tide.

C-CORE was involved with strain measurement in the ice cover, while The Hamburg Ship Model Basin (HSVA) has carried out in situ stress measurements in the ice cover.

5.3.1 Site description

The area of investigation was at the intersection of Lancaster Sound and Navy Board Inlet (73°45'N, 81°30'W) as shown in Figure 27. Lancaster Sound, the eastern entrance to the Northwest Passage, extends from Baffin Bay into the islands of the Canadian Arctic. There is a general movement of ice through Lancaster Sound from west to east under the action of wind and current.

Navy Board Inlet is a fiord-like feature, which also connects to Baffin Bay through Eclipse Sound and Pond Inlet. Lancaster Sound and Navy Board Inlet have water depths reaching 800 and 400 m, respectively. A sill at their intersection does not exceed 200 m depth and, for the most part, is less than 100 m deep. The maximum water depth between Adams Island and the Borden Peninsula is 30 m. The tidal range is about 1.5 m. Adams Island is situated about 3 km offshore from a base camp (Borden Station) on the Borden Peninsula (*Frederking at al., 1986a*).

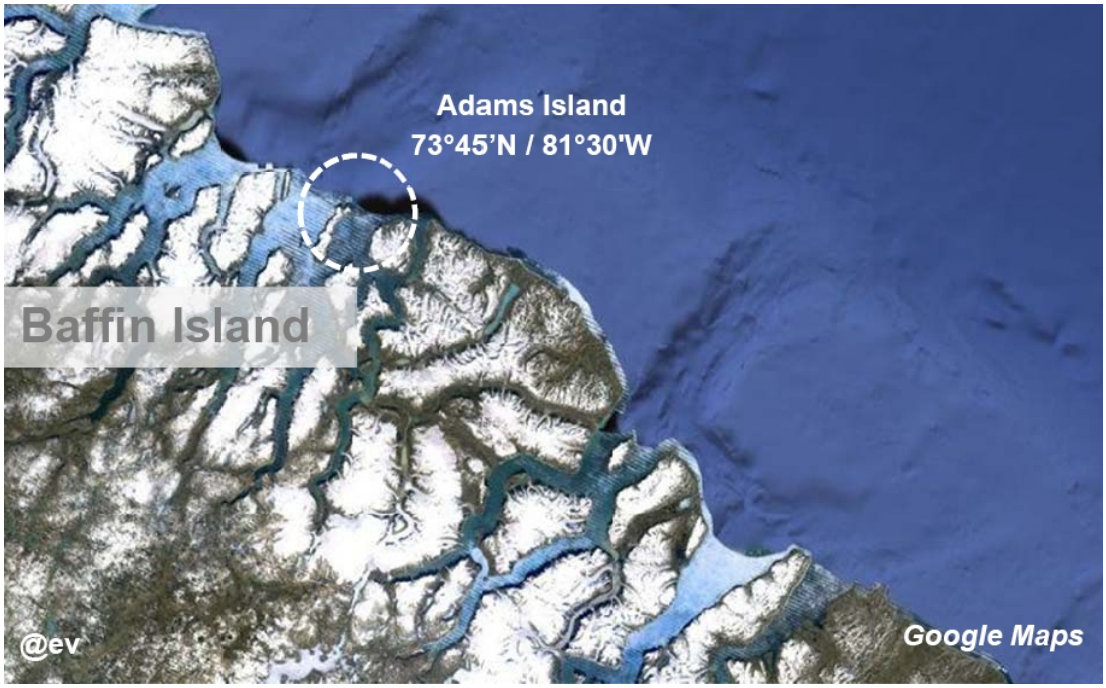

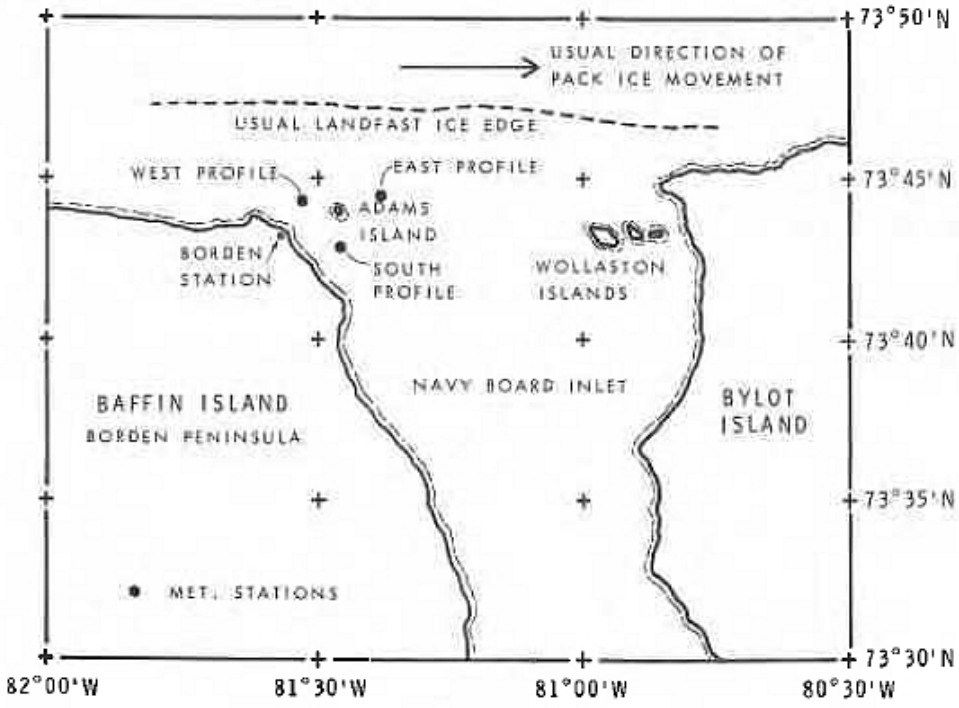

Figure 27 Location map of study area Adams Island

5.3.2 Ice conditions in the Lancaster Sound area

First-year ice normally forms in the middle part of Navy Board Inlet in October, becomes landfast, and progresses northward up the Inlet, reaching Lancaster Sound in November.

The island is generally at the boundary between level and ridged ice. Shear and pressure ridges make up a zone of ridged ice, which becomes landfast ice in mid-winter to a distance of about 5 km north of the island.

During the open-water season, multiyear ice from the Arctic Archipelago moves through Lancaster Sound to be discharged into Baffin Bay.

Icebergs from the glaciers of Greenland and Ellesmere Island circulate in the Sound. Some of these bergs pass into Navy Board Inlet and are frozen into the ice cover while others ground on the sill at the entrance to the Inlet. Typically there can be 5 to 10 large icebergs within 10 km of Adams Island. Multiyear ice is also frozen into the ice cover and may reach coverages of 1-5% (*Frederking at al., 1986a*).

The ice pack in Lancaster Sound is generally dynamic throughout the entire winter, although there have been occasions when it has frozen over completely (*Dey,1981*), as was the case for the winter 1982/1983.

5.3.3 Stress measurements

Figure 28 shows the history of stresses measured with stress panel and the temperature in the panels.

The results from the two types of ice pressure measuring transducers are similar. The panel was oriented about 50° clockwise from north and the orientation of the major principal stress from the biaxial transducer was about 65° clockwise from north. Therefore the biaxial transducer should yield higher stresses (*Frederking at al., 1986a*).

The general pattern of the stresses is similar, i.e., maximums for March 15-18, March 25-28, and April 14- 17, and minimums for March 23-24, April 4-9, and April 25-26.

The absolute maximum stress recorded with the panel was 250 kPa and the maximum average stress through the top 1.5 m of the ice cover was 150 kPa.
With the biaxial transducer the maximum stress was 350 kPa and the maximum average stress through the ice cover was estimated to be 250 kPa. These average stresses are higher than the 120 kPa determined at the same site in the spring of 1983 (*Frederking et al. 1984*).

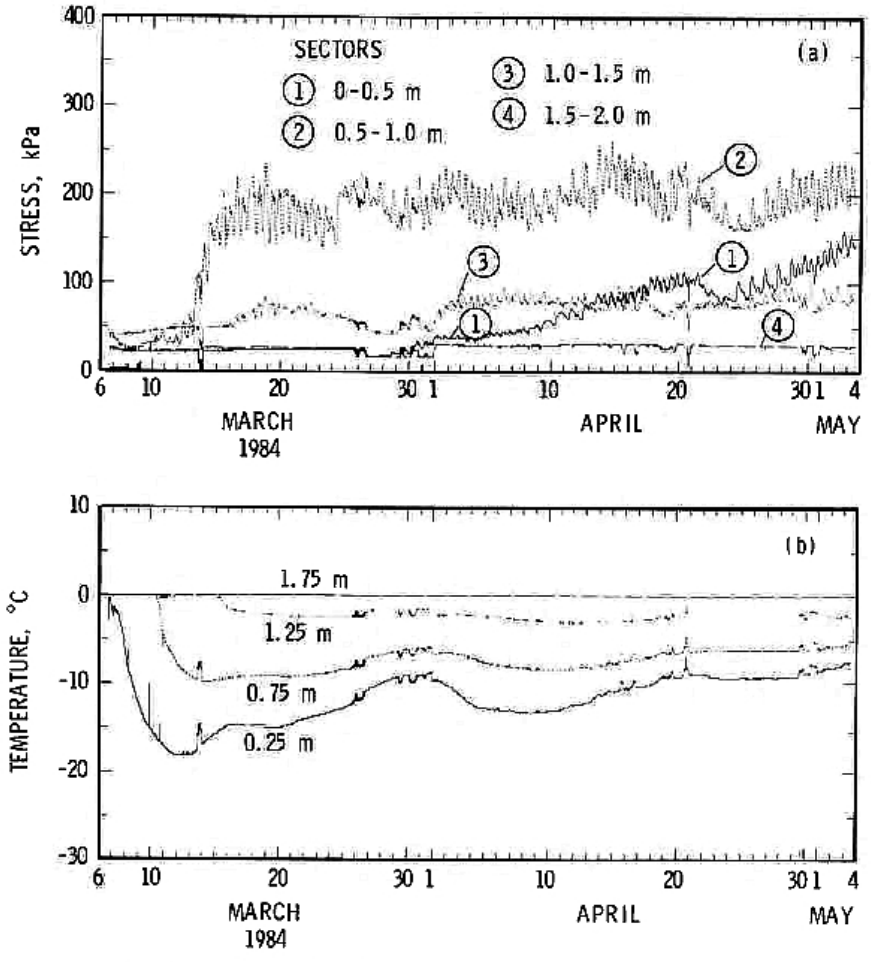

Figure 28 (a) Stresses measured in each sector of a 1 x 2 m stress panel, (b) Temperatures in stress panels at different depth from ice surface, Period: March – May 1984, (*Frederking et al., 1986a*)

For a shorter period, tide and stress have been plotted on an expanded time base to illustrate the relation between them (Figure 29). The stress peaks occur at low tide and the minimums at high tide. There is also a secondary peak halfway between high and low tide, a time at which the current velocity would be at a maximum.

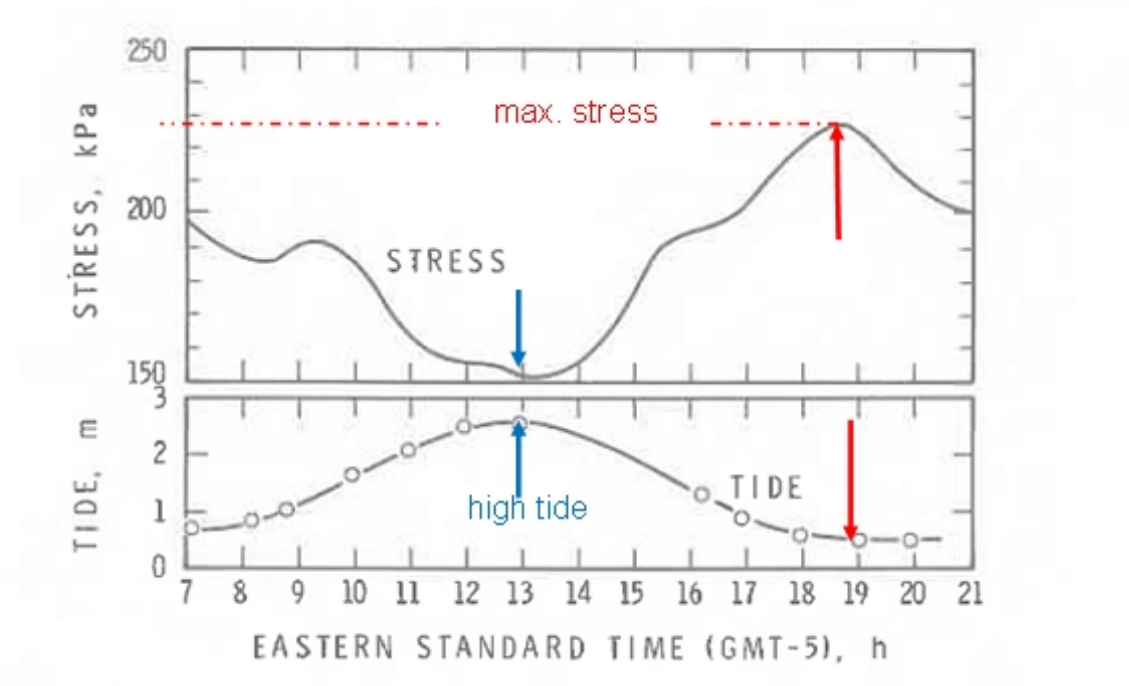

Figure 29 Example of measured tide and stress in sector 2 (0.5 -1.0 m from top surface) of stress panel, March 18, 1984 (after *Frederking et al., 1986a*)

5.3.4 Results obtained during the field campaign Adams Island winter 1983/84

Horizontal movements of the landfast ice cover adjacent to Adams Island show regular patterns on a spacial and temporal basis. Rates varied from 20 mm/day up to 300 mm/day with an average of about 100 mm/day. Movement direction was between north and northeast from November 1983 until May 1984.

Wind, air temperature, current, and tide all have an influence on ice movements but an adequate explanation for the coupling of these factors to ice movement was not evident at this time.

The maximum stress levels appear to be concentrated in the top half of the ice cover and related to temperature change in, and movements of, the ice cover. The maximum average stress measured on approximately 1.5 m thick, slowly moving landfast ice cover adjacent to Adams Island in the March to May 1984 period was about 250 kPa.

The results of this investigation indicate that in areas with ice conditions similar to those of the study area, i.e., landfast first-year sea ice moving at rates of 0.3 m/day or less, the maximum winter ice pressure on a wide structure (200 m) is 250 kPa (equivalent load of 90 MN for 1.8 m thick ice).

Note: The above mentioned results should not be used directly as design ice loads but they are a reasonable reference against design loads can be compared.

5.3.5 Results obtained during the field campaign Adams Island winter 1984/85

The field study at Adams Island carried out in winter 1983/84 was continued in winter 1984/85. The investigations were focused again on the measurement of ice stresses.

Figure 30 shows a record of the stress panel and the predicted tidal range. Obviously there is a significant shot-term periodicity (12.5 hours) in the results, which corresponds to the semi-diurnal tidal cycle, the stress peaks corresponding to the low tide. Similar periodicity was observed on all stress panels. (*Frederking et al., 1986b*).

It is also evident that the amplitude of the stress variation increased and decreased with the tidal range.

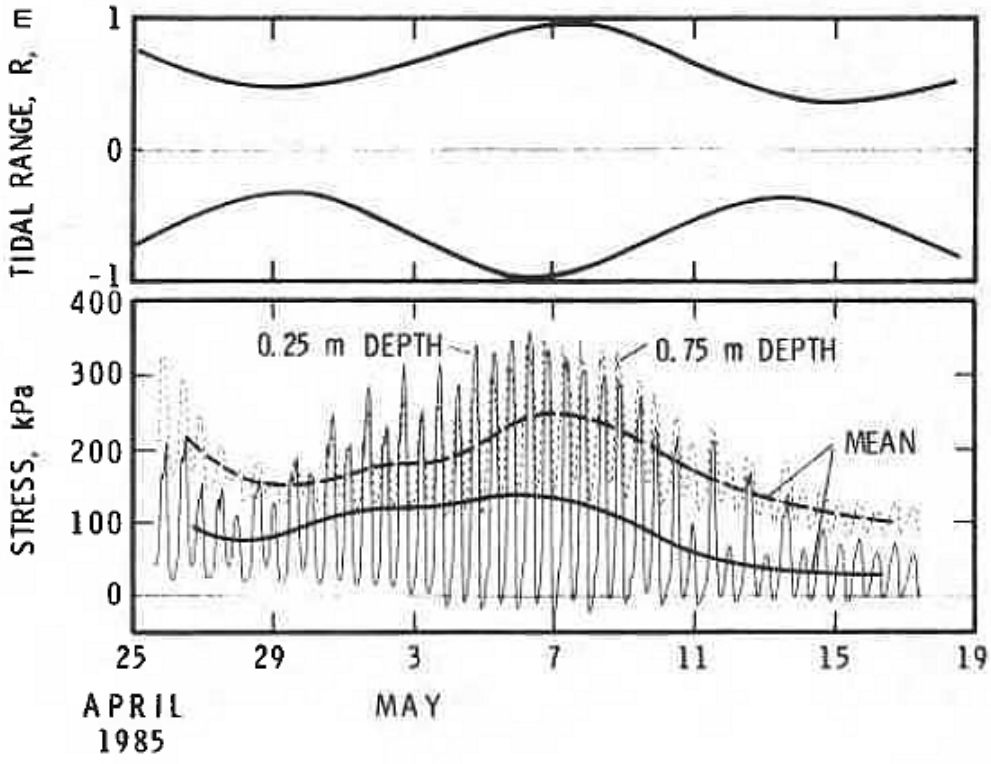

Figure 30 History plot of stress panel and predicted tidal range (period 25 April – 19 May 1985 (*Frederking et al., 1986b*)

The results of this field campaign winter 1984/85 can be summarized as:

- Tidal variations appear to be responsible for the horizontal ice cover movement rates and hence cyclical variations in the ice stresses.
- Displacement measurements have shown that the average horizontal ice movement rate is directly proportional to the tidal range.
- It was found that current, wind and air temperature also affect ice movements and stresses.
- The maximum total ice load generated on the island was about 60 MN, which is equivalent to an average ice stress of 300 kPa over the top 1 m of ice thickness and 200 m width.

- Local ice pressure acting on a 0.5 m^2 area reached a maximum stress of 500 kPa.

5.3.6 Stress measurements in Van Mijenfjorden (Svalbard), 6 - 11 May 2007

Ice stress measurements were carried out in the vicinity of a breakwater in Sveabukta, the innermost bay of Van Mijenfjorden (Svalbard), built for research purposes (see Figure 31).

The breakwater is 50 m long, 25 m wide and has a freeboard of about 2 m above mean sea level (MSL), which is taken as the reference level. The depth at the toe is 3.5 m and the slope is 1:2.5. During winter period several cracks were formed in the ice parallel to the breakwater up to a distance of 25 m. Stress sensors were deployed on each side of a crack, which is oriented 46° to the North. The ice cover was 1.6 m thick.

The sensors were deployed as two rosettes on each side of the crack at a depth of 0.18 m. These sensors consist of a disc of 10.5 cm in diameter filled with hydraulic oil and a transducer head measuring the voltage difference. Compressive stresses are obtained with ± 0.1 kPa resolution. Tensile stresses are not measured.

The centre of the rosettes was at a distance of 30 cm from the crack. In both rosettes, one sensor measured stresses perpendicular to the crack (Figure 31 (b)) and the angle between each sensor was 120 degrees as shown in Figure 31 (c) (*Caline and Barrault, 2008*)

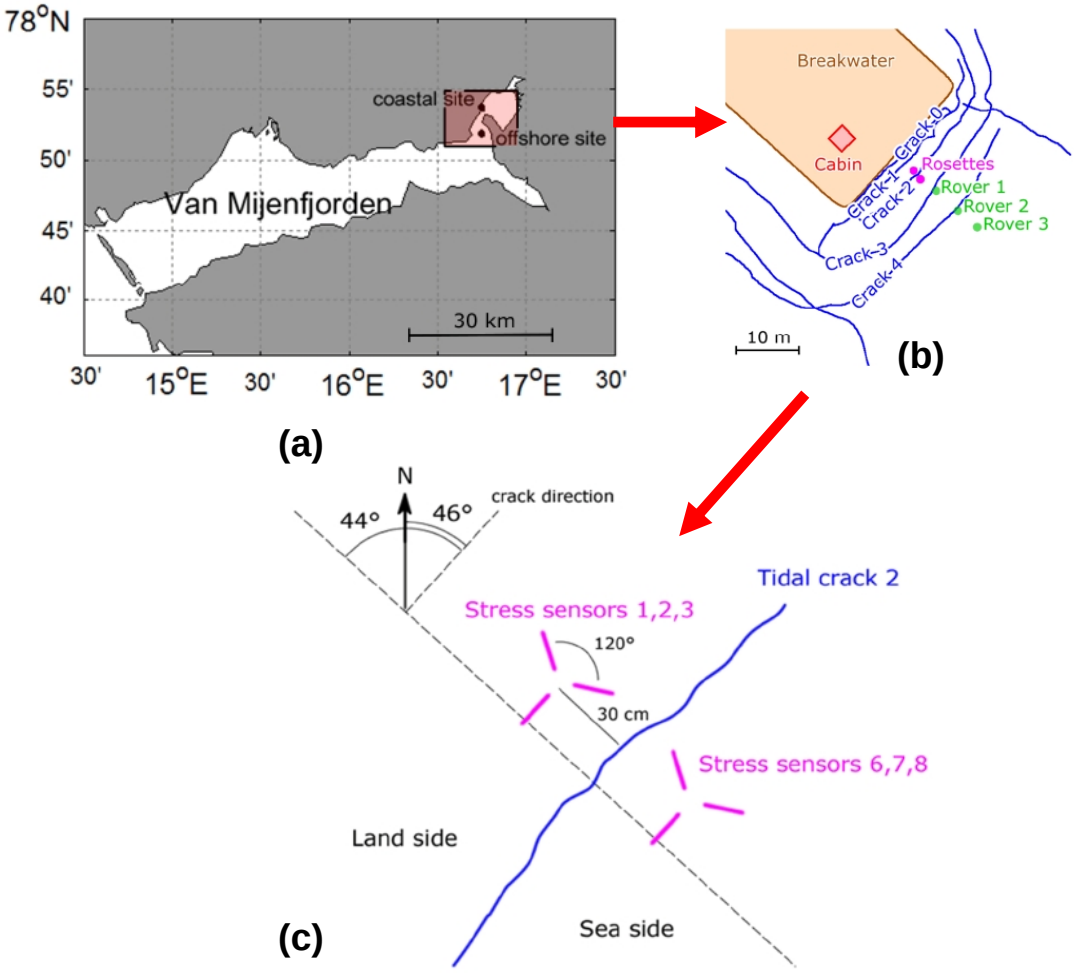

Figure 31 Measurement site and instrument set-up at Sveabukta in van Mijenfjorden (after *Caline and Barrault, 2008*)

In Figure 32 a history plot of stresses [kPa], air temperature [°C] and water level [m] is presented.

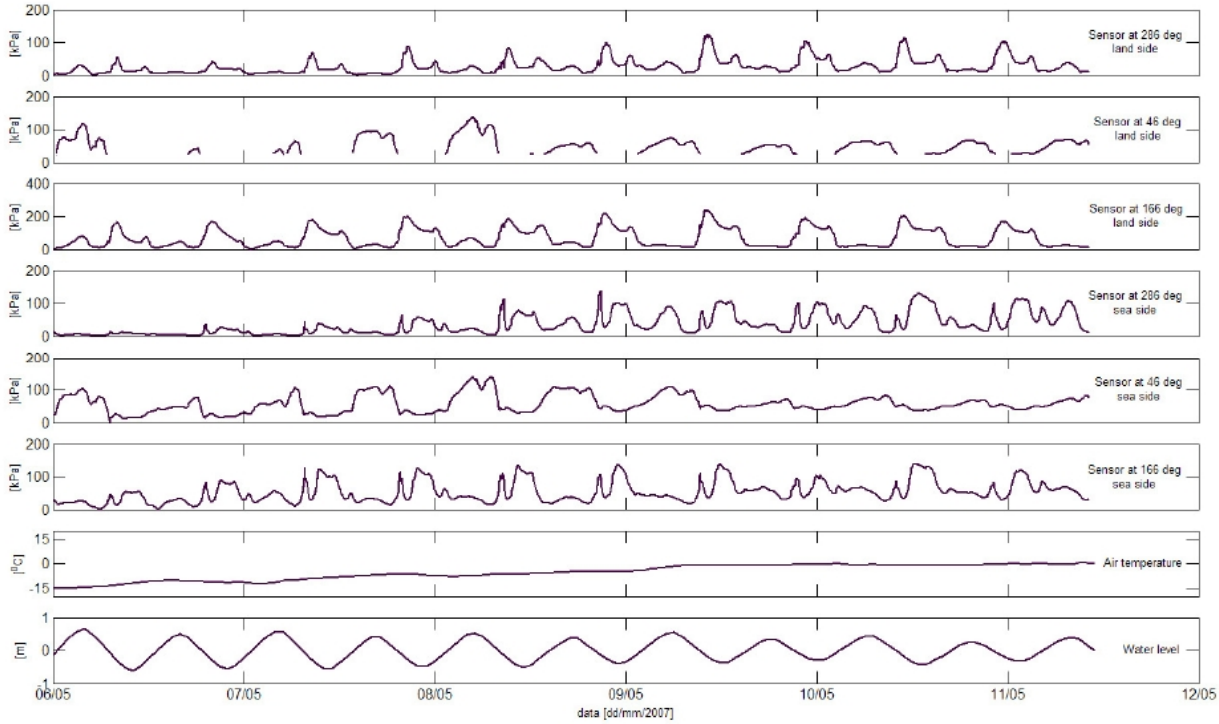

Figure 32 History plot of stresses [kPa], air temperature [°C] and water level [m] (*Caline and Barrault,, 2008*)

The results can be summarized as:

- As shown in Figure 2 stresses were identified as periodic events on both sides of the crack with higher pressure on the land side of the crack with a maximal value of 245 kPa compared with 139 kPa on the sea side.

- The stresses are strongly influenced by the tide and their tidal response is similar during the whole week.

- During the 6 days of measurements the temperature increased almost linearly from -15 to 0°C.

- The wind was around 11 ms^{-1} until 9 May then decreased to 5 ms^{-1}. All the time the wind was from the northeast direction, i.e. parallel to the tidal crack. The tidal range decreased from 1.26 m on 6 May to 0.56 m on 11 May.

5.4 Vessels in compressive ice

When a ship is proceeding in compressive ice where the driving force and thus the largest principal stress is normal to the ship track, the channel broken by the vessel begins to close rapidly after the vessel has passed. If the edges of the closing ice sheet get in contact alongside with the ship, forces increases and most likely the ship stops.

As an example Figure 33 shows the MV *Tornedalen* that got stuck in compressive ice in the Baltic Sea and Figure 34 shows the vessel *Akademik Shokalskiy* trapped in ice during the *Australasian Antarctic Expedition* in December 2013. .

Figure 33 Motor vessel MV *Tornedalen* getting stuck in compressive ice in the Baltic Sea

ICE-STRANDED EXPLORERS' MESSAGE:

A statement from the Australasian Antarctic Expedition:

We're stuck in our own experiment. We came to Antarctica to study how one of the biggest icebergs in the world has altered the system by trapping ice. We followed Sir Douglas Mawson's footsteps into Commonwealth Bay, and are now ourselves trapped by ice surrounding our ship.

Sea ice is disappearing due to climate change, but here ice is building up. We have found this has changed the system on many levels. The increase in sea ice has freshened the seawater below, so much so that you can almost drink it. This change will have impacts on the deep ocean circulation.

Underwater, forests of algae are dying as sea-ice blocks the light. Who can say what effects the regional circulation changes may have on the ice sheet of the Antarctic plateau, or whether the low number of seals suggests changes to their population.

(ref. http://wattsupwiththat.com)

Figure 34 *Akademik Shokalskiy* trapped in Antarctic ice for two weeks during the *Australasian Antarctic Expedition* in December 2013

For the development and design of icebreaking vessels operating in the Arctic on the one hand and for Ice Route Optimization (IRO) on the other hand it is important to investigate how these ships would be affected by compressed ice.

Because there is only limited information about ice compression, physical model tests in ice tanks were carried out in order to study the behavior of vessels in broken channels and in pressurized ice fields.

In general winds and currents are causing horizontal loads on the ice cover – these loads are causing the ice drift. When drifting ice is meeting a boundary, shoreline, then first the natural or artificial leads are closed.

When the ice has reached 100 % (10/10th) coverage, ridge formation may start when the driving forces are still high enough. During the ridge is forming stresses in the ice field develop. When a vessel is passing through an area where the ice cover is under compression (high internal ice stress), the broken channel left behind the ship starts to close immediately.

As the bow of the vessel is breaking a channel only slightly wider than the vessel itself, the moving ice field may encounter the vessel at the mid-body as demonstrated schematically in Figure 35. In this situation the ice resistance is increasing significantly.

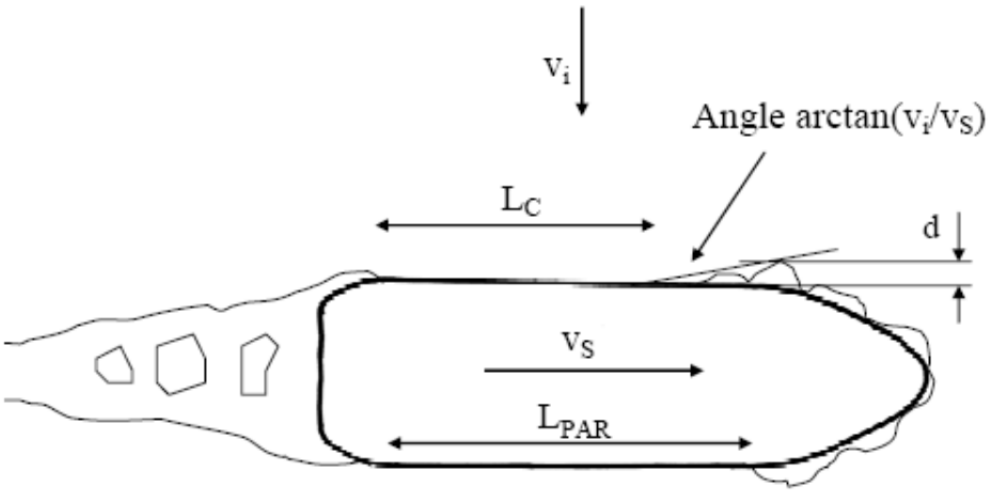

Figure 35 Schematic diagram of a vessel navigating through compressive ice. The ice drift direction is normal to ship track direction (*Riska et al., 2006*)

A critical situation often arises when the channel behind the ship closes and the ship is not able to move astern. However, this manoeuvre is often required during ramming of massive ice ridges.

Equally important is the consideration of the additional ship resistance due to compressed ice that restricts the maneuverability of the vessel. The added resistance is mainly depending on the ice line load and ice drift speed perpendicular to the ship.

Riska et al., 2006 proposed a formula to estimate the total resistance in compressive ice (R_{iTC}). This formula is based on the length the ice is in contact with the parallel mid-body of the ship (L_C), the margin that the broken channel is wider than the vessel (d), the ship speed (v_s) and the ice drifting ice speed (v_i). If the compressive force in the ice field is assumed to be line force q (unit kN/m), then the ship resistance - assuming that Amonton's law (i.e. $q_\mu = \mu_q$) is valid - is:

$$R_{iTC} = R_{iT} + 2\, L_C\, q_\mu = 2\, [\, L_{PAR} - (v_s / v_i)\, d\,]\, \mu\, q$$

where

R_{iTC}	total resistance in compressive ice
R_{iTC}	total resistance in similar ice without compression
L_{PAR}	length of the ship's parallel midbody
L_C	contact length with parallel mid-body
v_s	ship speed
v_i	ice drift speed
d	margin that the broken channel is wider than the vessel
μ	friction coefficient
q	line force (unit kN/m)

5.4.1 Ice model tests conducted at HSVA

During the tests with lateral pressure two different ship models were tested. Both of them are designed in order to operate in ice covered seas but with different ice breaking capability.

Model A

- The first ship is an ice breaking container vessel of 184 m length. It is 29 m in breadth and operates at a design draft of 9.5 m. The two azimuth propulsors are driven by two 13 MW engines. The propellers are two four blade ice propellers with a diameter of 5.6 m. The vessel is able to break 2 m ice with a snow layer of 0.2 m at more than 2 knots ahead and astern. The ship's scaling factor is 28.

Model B

- The second ship is an ice breaking multi-purpose vessel. It has a length of 156 m, a breath of 28 m and it is operating on a draft of 7.5 m. This vessel is equipped with two azimuth propulsors with a diameter of 5.1 m. They are driven by a total engine power of 15 MW. The ship is able to break 1.2 m ice with a snow layer of 0.24 m ahead and astern at 2 knots. The ship has a scaling factor of 22.

Compressive ice model tests

In order to produce a corresponding lateral pressure in the ice sheet during the experiments, 3 pressure frames were installed along the wall of the ice tank (see Figure 36). Each frame has a length of 6 meter and was supported by two 2-way pneumatic cylinders. The stroke of a pressure cylinder is 0.2 m and it is adjustable in pressure and back pressure. That makes it possible to set the velocity and the force on the desired level. Each cylinder is equipped with a load cell measuring the applied force. Further the speed of the stroke was adjusted by a control valve and monitored by a video camera. The maximum stroke velocity was defined in a way that the channel is closed approximately two ship length behind the ship. The "overbreak" d of the ship model (see Figure 35) along its parallel midship is defined by the ice floe

broken at the ship's front shoulder. This "overbreak" was about 0.1 m for the investigated ship models. During a test all pressure cylinders were set to the same value. The force of pressure frames were adjusted from 240 N up to 1350 N. This is equivalent to a full scale line load of 40-200 kN/m.

A schematic diagram showing the acting forces on the ship is illustrated in Figure 37.

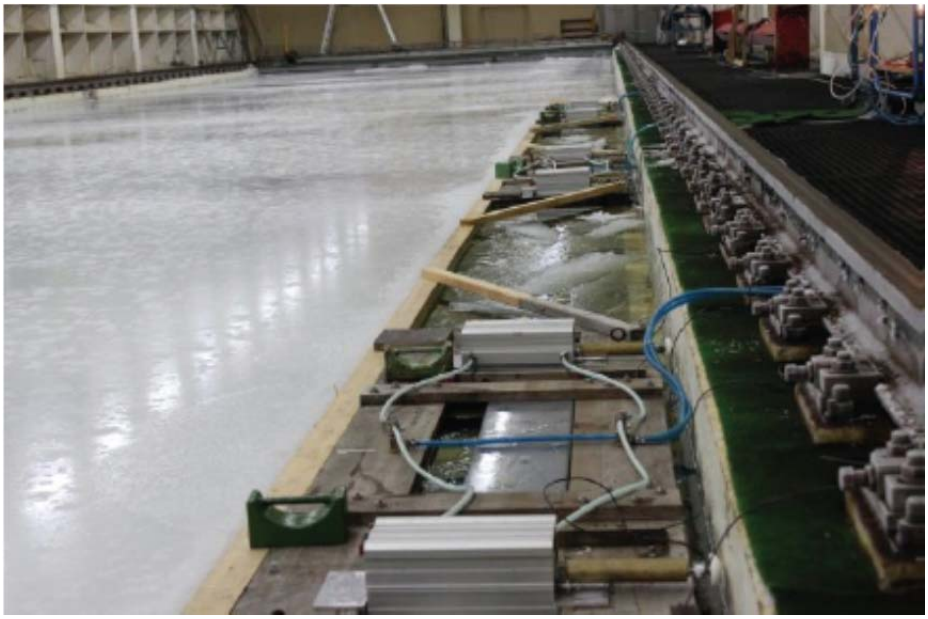

Figure 36 Pressure frames installed along the wall of ice tank

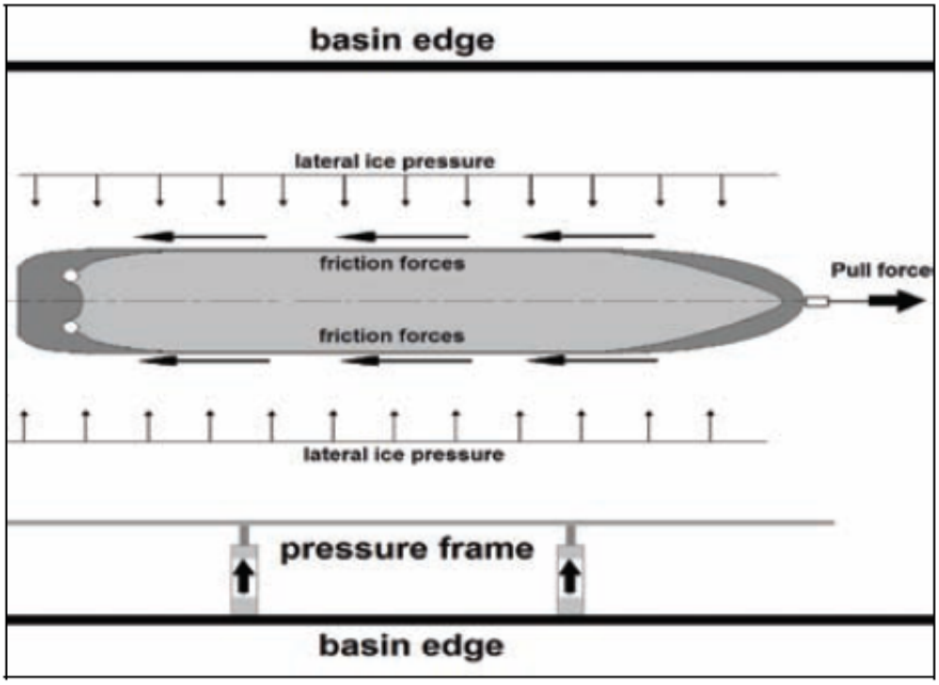

Figure 37 Schematic diagram of the forces acting on the ship in a resistance test

Resistance Test in Pre-Cut Level Ice

For the “pre-cut level ice” tests the ice was rearranged and the testing distance was shortened (Figure 38). Cuts were made between the pressure frames which made it possible for the cylinders to get out earlier than during the towed resistance tests in level ice. The ice behind the pressure frames was braced by wooden frames which have a negligible influence on the tests but were needed to close the ice surface.

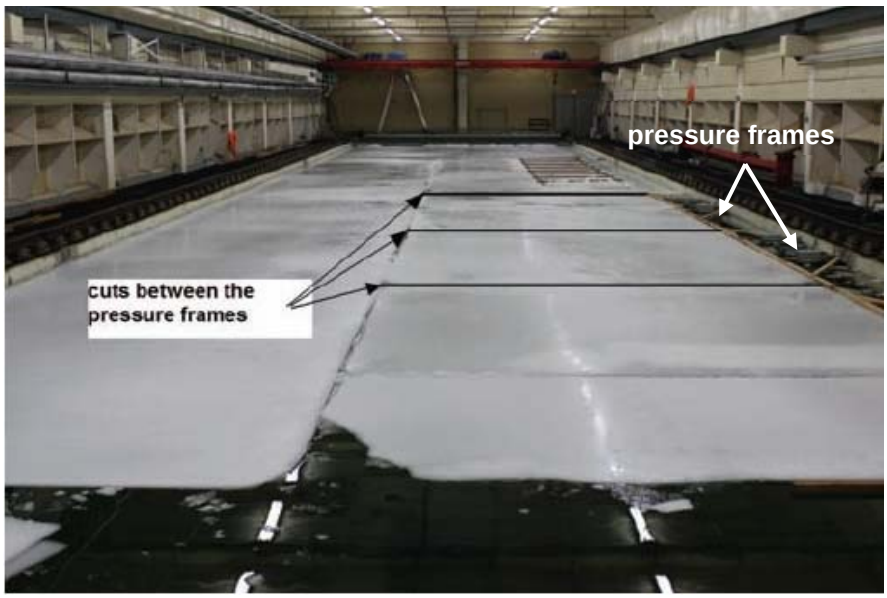

Figure 38 Ice sheet prepared for the “pre-cut “ level ice tests

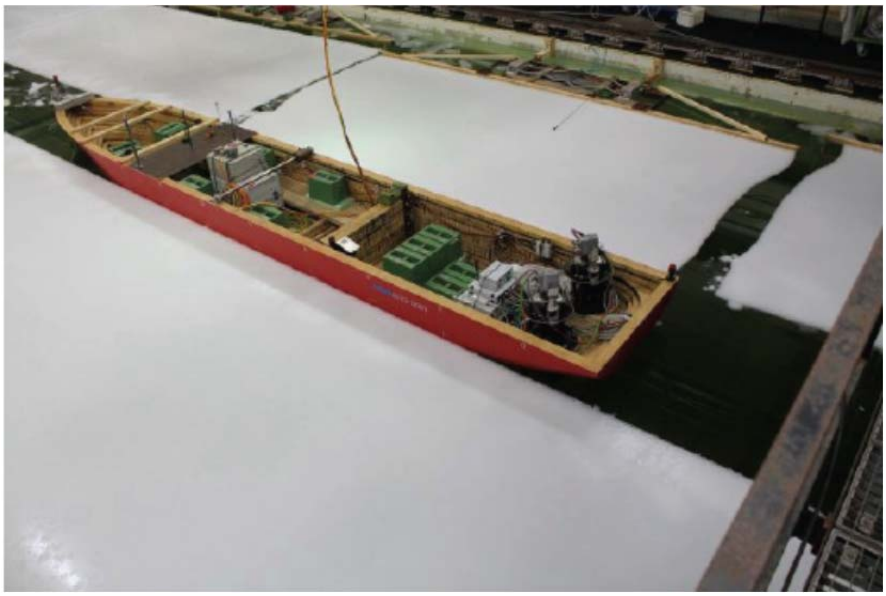

Figure 39 Model in pressured ice

Summary of test results

In Figure 40 the added resistance is plotted versus the lateral pressure (level ice test). Four different velocities of ships are shown for different pressure levels. All

model tests were performed in level ice. It is evident that the added resistance increases with decreasing speed.

If a long shear crack in level ice occurs, the boundary ice conditions are similar to the pre-cut tests. The results of level ice tests with long shear cracks were also taken into account for the analysis of the pre-cut tests.

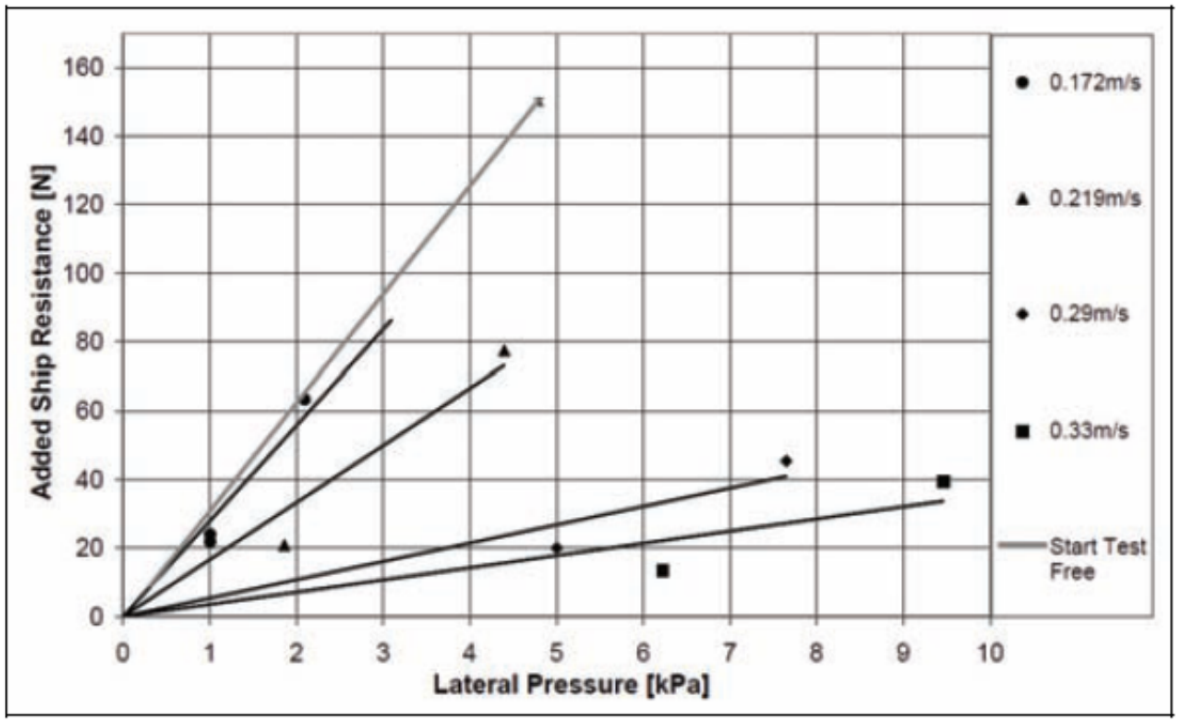

Figure 40 Added resistance versus lateral ice pressure, level ice test (model scale values)

In Figure 41 the added resistance is plotted versus the lateral pressure (pre-cut level ice test).

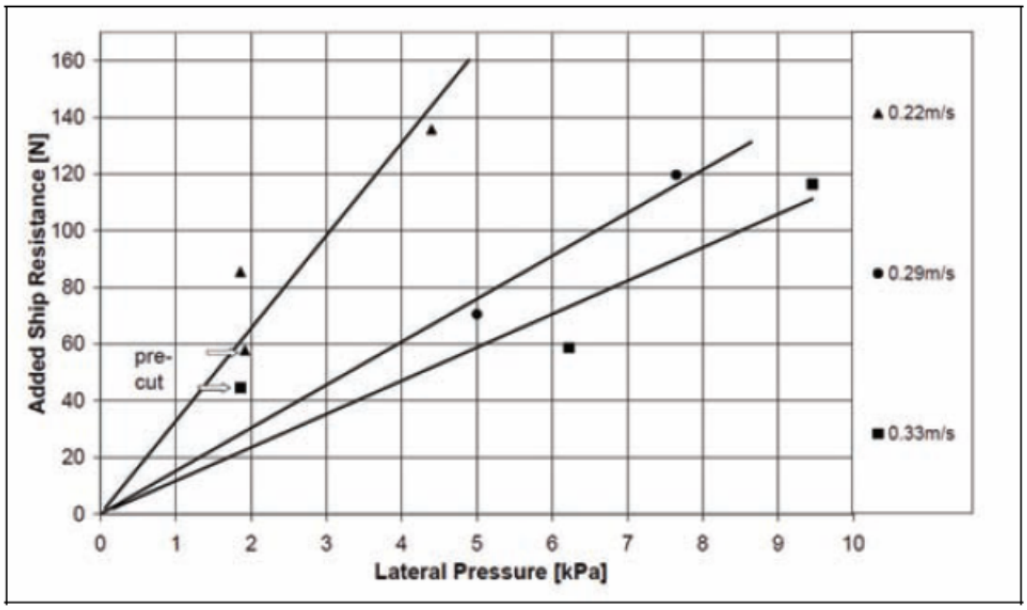

Figure 41 Added resistance versus lateral ice pressure, pre-cut test (model scale values)

The added resistance in pre-cut tests is higher than in level ice. It can be concluded from Figure 41 that the added resistance depends on the velocity but not as strong as in intact level ice which is not pre-cut.

By analyzing the gradients of the best fit lines of Figure 40 and Figure 41, the added resistance both in level ice and pre-cut ice can be calculated approximately:.

Added ship resistance in level ice :

$$\Delta R = (0.3\, e^{-13.46v})\, p$$

Added ship resistance in pre-cut level ice :

$$\Delta R = (0.25\, e^{-9.5v})\, p$$

where

ΔR added resistance

v ship speed

p lateral pressure

The formulas give a first approximation for ships with a similar bow form and length of the parallel midship acting in the same range of velocities and line-loads.
The calculated and measured added resistance versus ship speed is shown in Figure 42.

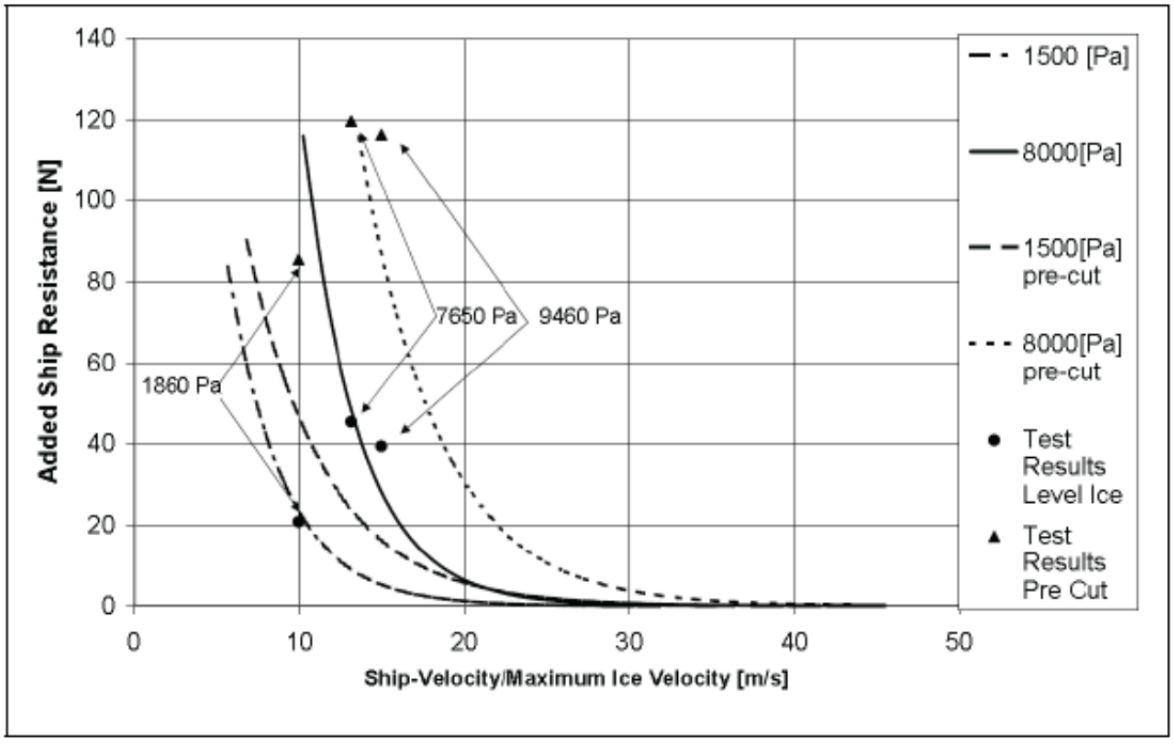

Figure 42 Comparison of calculated and measured added resistance

Assuming ice conditions prevailing in the field measurement campaigns carried out in the Beaufort Sea by *Richter-Menge et al*., in Adams Island (Lancaster Sound) by *Frederking et al*. and in Van Mijenfjorden (Spitsbergen) by *Caline et al*. the capability of a ship passing through compressed ice can be estimated by using the diagram in Figure 43.
The curves in the diagram are only valid for an assumed ice friction coefficient of C_{IF} = 0.1. At a higher coefficient of friction, the ice thickness, which can just be broken by the ship, is lower.

Example

The diagram gives an estimation, how the research vessel RV Polarstern, having a maximum bollard pull of 1.8 MN (friction coefficient C_{IF} = 0.1), can sail in pressurized ice.

Assuming a lateral ice pressure p=150 kPa the ship is able to break up to 1.2 m thick ice, when the lateral ice pressure increases to 200 kPa the ice thickness decrease to 0.9 m and for p = 250 kPa the vessel get stuck in 0.7 m thick ice.

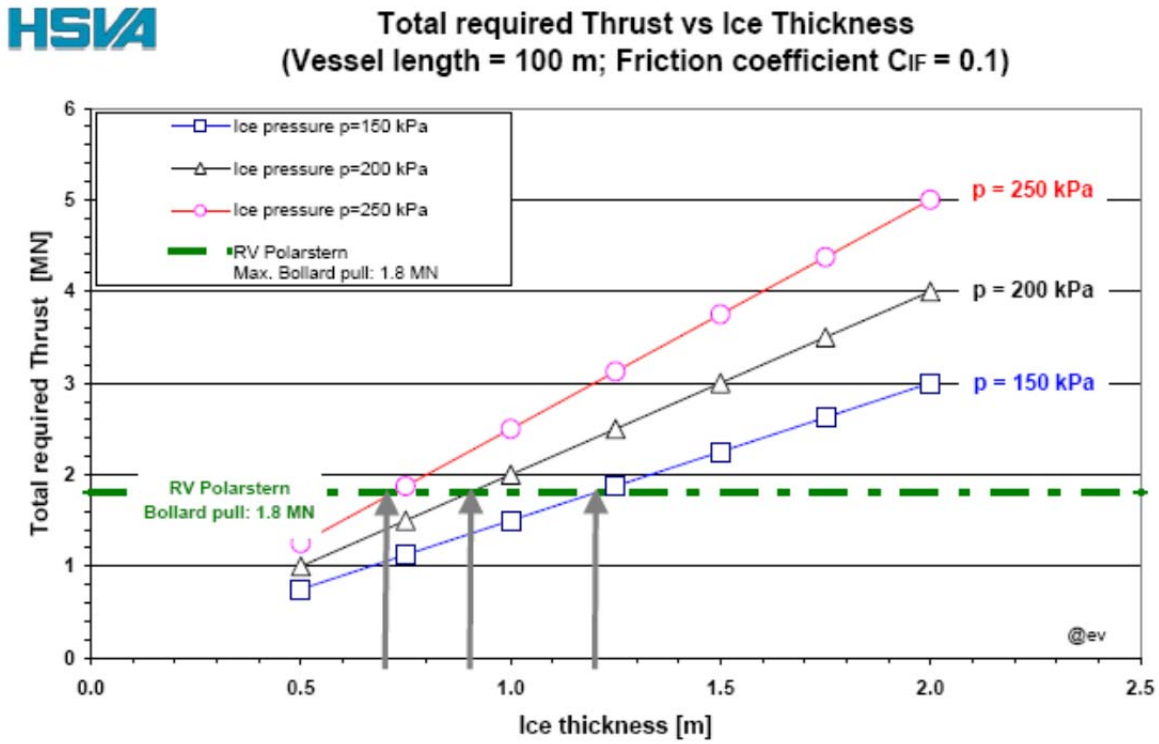

Figure 43 Total required thrust versus ice thickness in compressed ice

The objectives of the model tests were to investigate the influence of lateral pressure on ships resistance. It can be summarized :

- The velocity of a ship in compressive ice has a significant impact on the resistance.

- The model tests have shown that it is difficult to set small ice floes in the model basin under lateral pressure since the ice floes rafted when the pressure increases.

- There is a good correlation between the calculated and measured channel width. shows a well accordance to calculated values.

- The influence of the added resistance can be approximated by the given equations to calculate ΔR, because they show how different velocities will change the resistance and thus the required power of a vessel.

- The test results will be used to further improve the route optimization tool. However, in order to extend the amount of evaluated ship parameters and boundary conditions further research and model test performance is necessary.

This section 5.4.1 gives a general overview only, thus the reader is advised to study the relevant literature *Hinse (2013)* and *Hinse et al.,(2013*) for more detailed information.

6 Summary and Conclusions

The Hamburg Ship Model Basin (HSVA) together with the Scottish Association of Marine Science (SAMS) has developed in cooperation with Terrascience Systems Ltd., Canada an ice stress sensor system to be frozen in level or pack ice in the Arctic during the ACCESS WP 1 expedition organised by SAMS.

The objectives were to get lateral ice pressure data together with environmental information, temperature, wind speed and direction, current etc. and position of the ice stress sensors that should be transmitted via satellite onshore. Available meteorological and oceanographic data and satellite pictures should be used to gather information on the dependence of the ice pressure on environmental parameters. The goal was to use the collected data for improvement of the ICEROUTE- transit model. In WP1 the data should be used to benchmark the ice prediction models with respect to ice pressure.

During the design phase of the Lateral Stress Buoy (LSB), it became evident that the production of the measurement system is too expensive. Due to the high weight of the LSB, problems regarding transportation, handling and insertion into the ice, high costs were expected. It was also recognized that timely completion could not be guaranteed. For these reasons, it was decided in consultation with the leader of WP 2, not to pursue the development of this measurement system and to search for an alternative.

As an alternative ice force panels (IFP) from the company Terrasciences Ltd. in Canada were selected. About this idea the European Commission, Directorate-General for Research and Innovation was informed and a reallocation of funds for production of equipment in Task 2.51 has been requested. This application was approved by the EU scientific officer, who is responsible for the collaborative ACCESS Project no. 265863 – Arctic Climate Change, Economy and Society.

The IDEAL ice force panels (IFP) are custom-made manufactured according to the specifications given by HSVA and should be used during the Arctic Expedition Winter 2013/14 in Fram Strait with research vessel RV Lance.

The plan was to use the ice force panels during the expedition towards northeast Spitsbergen where RV Lance will freeze in level or pack ice and move with the transpolar drift towards the Fram Strait.

Based on a decision of the Norwegian Research Council, the expedition could not be performed. This message was achieved during the ACCESS General Assembly meeting in Villanova in March 2013 and it was decided to use the IDEAL IFP during the Ice Camp field campaign in the Beaufort Sea in March 2014 organized by SAMS. The equipment was shipped to Sachs Harbour, Canada and deployed in sea ice by SAMS.

A fault in the internal SD card-holder of IFP data acquisition unit meant that no data was recorded during the Ice Camp field campaign. This is particularly disappointing because on the one hand it was possible to design and produce the ice stress measurement system and on the other hand, all constructive, technical, and logistical preparations were carried out for this Ice Camp campaign with huge effort to investigate the lateral pressure in Arctic sea ice.

In addition, a literature review regarding lateral ice pressure, which was not originally part of the ACCESS WP 2 Task 2.51 was performed.

The results of the literature study can be summarized briefly: In various field measurements campaigns carried out in Arctic sea ice (e.g. Beaufort Sea, Lancaster Sound and Spitsbergen) lateral ice pressure in the range of p = 150 kPa to 300 kPa was determined.

Because there is still too little information about temporal and spatial evolution of the ice pressure field, it is highly recommended to perform interdisciplinary field campaigns with geophysicists, meteorologists, oceanographers and ice engineers in the Arctic in the future. In such a campaign a better understanding of the lateral pressure of the ice can be obtained by use of complementary data sets.

New insights can be gained to what extent the climatic development in the Arctic in recent years has affected the internal pressure of the ice these days.

7 References

Abdelnour, R., Comfort, G., Singh, S., and Paterson, B.,1997. Pack Ice Pressure Forecasting for Arctic and Sub-Arctic Regions, 16th International Conference on Offshore Mechanics and Arctic Engineering (OMAE 1997), April 13 – 18, Yokohama, Japan

Caline, F. and Barrault, S., 2008. Measurements of stresses in the coastal ice on both sides of a tidal crack, 19th IAHR International Symposium on Ice "Using New Technology to Understand Water-Ice Interaction", Vancouver, British Columbia, Canada, July 6 to 11, 2008

Comfort, G., Ritch, R. and Frederking, R. M. W.,1992. Pack ice stress measurements in Proceedings of the 11th International Conference on Offshore Mechanics and Arctic Engineering, vo l. 4, edited by O. A. Ayorinde, et al., pp. 245-253, Am. Soc. of Mech. Eng., New York, 1992.

Comfort, G. and Ritch, R. 1990. Field Measurements of Pack Ice Stresses, Proceedings of the 10th International Conference on Offshore Mechanics and Arctic Engineering, Houston, Tx, USA

Coon, M.D., Lau, P. A. , Bailey, S. H. and Taylor, B. J., 1989., Observations of ice floe stress in the eastern Arctic, Proceedings of the 10th International Conference on Port and Ocean Engineering under Arctic Conditions, POAC'89, vol. 1, edited by K. B. E. Axelsson and L. A. Fransson, pp. 44-53, Lulea Univiversity of Technology, Lulea, Sweden, 1989.
Cox, G. F. N., and Johnson, J. B., 1983. Stress measurements in ice, Rep. 83-23, Cold Reg. Res. and Eng. Lab., Hanover, N.H., 1983.

Dempsey, J.P.,2000. Research trends in ice mechanics. International Journal of Solids and Structures 37,2000 131-153

Dey, B. B., 1981. Shipping routes, ice cover and year-round navigation in the Canadian Arctic, Polar Record, 20(129), pp. 549-559.

Frederking, R . M. W., and Evgin, E.,1990. Analysis of stress distribution in an ice floe, in Proceedings of the Ninth International Conference on Offshore Mechanics and Arctic Engineering, vol. 4, Arctic/Polar Technology, edited by O. A. Ayorinde, N. K. Sinha, and D. S. Sodhi, pp. 83-87, Am. Soc. of Mech. Eng., New York, 1990.

Frederking, R., E. Wessels, E., Maxwell, J. B., Prinsenberg, S., Sayed, M., 1986b. Ice Interaction with Adams Island, Winter 1984 – 85, Proceedings 8th International IAHR Symposium on Ice, Iowa City, Iowa, August 18 - 22,1986, Vol. III, p. 127-143

Frederking, R. M. W., Wessels, E., Maxwell, J. B., Prinsenberg, S., Sayed, M., 1986a.Ice pressures and behaviour at Adams Island, winter 1983/1984, Canadian Journal of Civil Engineering, 13, 2, pp. 140-49, 1986-04

Frederking, R.M.W., Sayed, M., Wessels, E., Child, A. J. and Bradford, D.,1984. Ice interaction with Adams Island, winter 1982- 1983. Proceedings International Association for Hydraulic Research Ice Symposium, Hamburg, West Germany, Vol. 3, pp. 187-201.

Frederking, R. and Nakawo, M. 1984. Ice action on Nanisivik wharf, winter 1979-1980, Canadian Journal of Civil Engineering, 11(4), pp. 996-1003.

Hallam, S. D., N. Jones, and M. W. Howard, The effect of sub-surface irregularities on the strength of multi-year ice, ASME J. Offshore Mech. Arc. Eng., 111,350-353, 1989.

Hinse, P., Ehle, D. and Reimer, N., 2013. Model Tests for Determination of Ship Resistance in Level Ice under Lateral Pressure, Proceedings of the Twenty-third (2013) International Offshore and Polar Engineering, Anchorage, Alaska, USA, June 30–July 5, 2013

Hinse, P. (2013). Model Tests for Determination of Ship Resistance in Level Ice under Lateral Pressure, Bachelor thesis BSC – 016, Institute for Mechanic and Ocean Engenieering, Technical University Hamburg-Harburg,

Johnson, J. B., Cox, G. F. N. and Tucker, W. B. III, 1985. Kadluk ice stress measurement program, Proceedings of 8th International Conference on Port and Ocean Engineering Under Arctic Conditions, Danish Hydraulic Institute, Horsholm, Denmark, 1985.

Richter-Menge, J. A., S. L. McNutt, J. E. Overland, and R. Kwok, 2002.Relating arctic pack ice stress and deformation under winter conditions, Journal of Geophysical. Research, 107(C10), 8040, doi:10.1029/2000JC000477, 2002.

Richter-Menge, J. A. and Elder, B.C. ,1998. Characteristics of pack ice stress in the Alaskan Beaufort Sea, Journal of Geophysical Research, Vol. 103, No. C10, page 21817-21829, September 15, 1998

Riska. K. Breivik, K., Eide, S.I., Gudmestad, O.T. and Hilden, T., 2006. Factors Influencing the Development of Routes for Regular Oil Transport from Dikson, ICETECH 06 - 7th International Conference and Exhibition on Performance of Ships and Structures in Ice Banff, Alberta, Canada 16-19 July 2006

Riska, K.,n.d. Design of Icebreaking Ships

Cold Regions Science and Marine Technology - Design of Ice Breaking Ships, Encyclopedia of Life Support Systems (EOLSS)

SukhorukovK, . K., Internal stresses at typical local inhomogeneities of sea ice cover, paper presented at 13th International Conference on Port and Ocean Engineering under Arctic Conditions, Am. Soc. of Mech. Eng., Murmansk, Russia, Aug. 15-18, 1995.

Tucker, W . B., III, and Perovich, D. K., 1992. S tress measurements in drifting pack ice, Cold Regions Science and Technology, 20, 119-139, 1992.

Tunik, A., 199.Impact Ice Pressure: More Questions than Answers, International Union of Theoretical and Applied Mechanics 1991, pp 693-714